# cmgh

ORIGINAL RESEARCH

The Hippo Kinase LATS2 Controls *Helicobacter pylori*-Induced Epithelial-Mesenchymal Transition and Intestinal Metaplasia in Gastric Mucosa

Silvia Elena Molina-Castro,[1,2] Camille Tiffon,[1] Julie Giraud,[1] Hélène Boeuf,[3] Elodie Sifre,[1] Alban Giese,[1] Geneviève Belleannée,[4] Philippe Lehours,[1,4] Emilie Bessède,[1,4] Francis Mégraud,[1,4] Pierre Dubus,[1,4] Cathy Staedel,[5] and Christine Varon[1]

[1]INSERM, UMR1053, Bordeaux Research in Translational Oncology, BaRITOn, [3]INSERM, UMR1026, Bioingénierie tissulaire (BioTis), [5]INSERM, UMR1212, University of Bordeaux, Bordeaux, France; [2]University of Costa Rica, San José, Costa Rica; [4]Centre Hospitalier Universitaire (CHU) de Bordeaux, Bordeaux, France
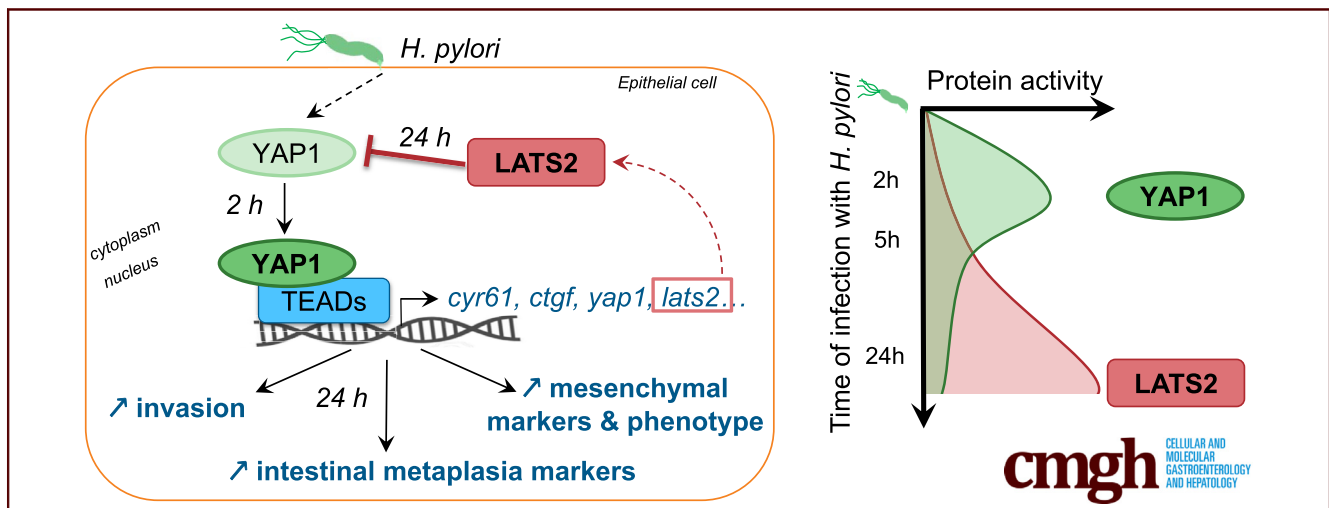
SUMMARY

The tissue homeostasis-regulating Hippo signaling pathway is activated during *Helicobacter pylori* infection. The Hippo core kinase large tumor suppressor 2 was found to protect gastric cells from infection-induced epithelial-to-mesenchymal transition and metaplasia, a preneoplastic transdifferentiation at high risk for gastric cancer development.

BACKGROUND & AIMS: Gastric carcinoma is related mostly to *CagA+-Helicobacter pylori* infection, which disrupts the gastric mucosa turnover and elicits an epithelial-mesenchymal transition (EMT) and preneoplastic transdifferentiation. The tumor suppressor Hippo pathway controls stem cell homeostasis; its core, constituted by the large tumor suppressor 2 (LATS2) kinase and its substrate Yes-associated protein 1 (YAP1), was investigated in this context.

METHODS: Hippo, EMT, and intestinal metaplasia marker expression were investigated by transcriptomic and immunostaining analyses in human gastric AGS and MKN74 and non-gastric immortalized RPE1 and HMLE epithelial cell lines

challenged by *H pylori*, and on gastric tissues of infected patients and mice. LATS2 and YAP1 were silenced using small interfering RNAs. A transcriptional enhanced associated domain (TEAD) reporter assay was used. Cell proliferation and invasion were evaluated.

RESULTS: LATS2 and YAP1 appear co-overexpressed in the infected mucosa, especially in gastritis and intestinal metaplasia. *H pylori* via CagA stimulates LATS2 and YAP1 in a co-ordinated biphasic pattern, characterized by an early transient YAP1 nuclear accumulation and stimulated YAP1/TEAD transcription, followed by nuclear LATS2 up-regulation leading to YAP1 phosphorylation and targeting for degradation. LATS2 and YAP1 reciprocally positively regulate each other's expression. Loss-of-function experiments showed that LATS2 restricts *H pylori*–induced EMT marker expression, invasion, and intestinal metaplasia, supporting a role of LATS2 in maintaining the epithelial phenotype of gastric cells and constraining *H pylori*–induced preneoplastic changes.

CONCLUSIONS: *H pylori* infection engages a number of signaling cascades that alienate mucosa homeostasis, including the Hippo LATS2/YAP1/TEAD pathway. In the host–pathogen conflict, which generates an inflammatory environment and perturbations of the epithelial turnover and differentiation,

Hippo signaling appears as a protective pathway, limiting the loss of gastric epithelial cell identity that precedes gastric carcinoma development. *(Cell Mol Gastroenterol Hepatol 2020;9:257–276; https://doi.org/10.1016/j.jcmgh.2019.10.007)*

The gram-negative microaerophilic bacterium *Helicobacter pylori* specifically colonizes the stomach of half the world's population, provoking a chronic inflammation of the gastric mucosa that most often is asymptomatic. However, 10% of infected persons sequentially develop, via a well-described process known as Correa's cascade, atrophic gastritis, intestinal metaplasia, and dysplastic changes that can evolve for less than 1% of the cases into gastric adenocarcinoma (GC).[1] GCs are the most frequent stomach cancers; it ranks third among cancer-related deaths worldwide.[2] *H pylori* strains positive for the *cag* pathogenicity island, which encodes a type 4 secretion system, and the virulence oncoprotein CagA, are associated strongly with gastric inflammation and malignancy.[3,4] Upon *H pylori* adhesion on human gastric epithelial cells, the type 4 secretion system forms a pilus, which translocates CagA and peptidoglycans into the epithelial cytoplasm, triggering cell innate immunity and other signaling pathways that alienate the mucosa homeostasis.[5,6]

Epithelial turnover, resulting from the balance between progenitor cell proliferation and differentiated cell death, is a major host defense mechanism against pathogens and recurrently is altered during bacterial infections and chronic inflammatory diseases.[5] In *H pylori*–infected gastric epithelial cell lines, we previously reported that *H pylori* via CagA blocks cell-cycle progression by up-regulating the cell-cycle regulator large tumor suppressor 2 (LATS2).[7] In addition, it elicits an epithelial-to-mesenchymal transition (EMT) involving the transcription factor Zinc finger E-box-binding homeobox 1 (ZEB1).[8,9] EMT is characterized by the loss of epithelial cell polarity and cell–cell interactions, reorganization of the cytoskeleton, and acquisition of the migratory properties of mesenchymal cells.[10] EMT may contribute to reduced renewal and aberrant differentiation of the gastric mucosa in *H pylori*–infected patients, leading to preneoplastic atrophic gastritis and intestinal metaplasia.[1]

The tumor suppressors LATS1/2, along with Mammalian Ste20-like kinases 1/2 (MST1/2) and their cofactor Salvador, constitute the kinase core of the Hippo pathway, an evolutionarily conserved signaling cascade involved in tissue homeostasis, organ size control, and cancers.[11] When the Hippo pathway is activated, thereby restricting tissue overgrowth, LATS1/2 phosphorylates the transcriptional coactivator YAP1 on serine-127, leading to its cytoplasmic retention and proteasomal degradation. On the contrary, when the Hippo pathway is inactive, nonphosphorylated YAP1 translocates into the nucleus and acts as coactivator for the transcription enhancer factors TEADs to promote cell survival and proliferation. The Hippo pathway interacts with other pathways such as Wingless Int (Wnt)/β-catenin,

Ras, junctional complexes, nuclear factor-κB (NF-κB), transforming growth factor β, and many others.[12,13] Some Hippo pathway effectors have been reported to be altered in tumors compared with normal tissue,[11,14] including GCs[15–17]: down-regulation of LATS1/2 along with overexpression of the oncogenic YAP1 in the nucleus are described most often and are associated with aggressiveness and a poor prognosis. The carcinogenesis processes related to *H pylori* infection are not fully understood, although several mechanisms have been deciphered.[18] Here, we aimed to explore the alterations of the Hippo pathway core constituted by LATS2 and its substrate YAP1 during *H pylori*–induced gastric carcinogenesis; the study of the LATS2/YAP1 tandem is a novel approach to the carcinogenesis induced by oncogenic bacteria. Therefore, we used gastric tissues of either patients or mice at characteristic stages of the Correa's cascade upon *H pylori* infection. We also used tissue culture systems of human gastric and nongastric epithelial cell lines to recapitulate in vitro the early events of *H pylori* infection occurring within an actively replicating gastric mucosa, and to perform infection kinetics and loss of function studies. We found an unexpected role of LATS2 in protecting host cells from *H pylori*–induced gastric EMT and intestinal metaplasia, a preneoplastic lesion that confers increased risk for GC development.

Results

LATS2 and YAP1 Are Co-Up-Regulated in the Gastric Epithelial Cells of H pylori–Infected Patients or Mice

LATS2 and YAP1 expressions were evaluated and scored by immunohistochemistry in the gastric mucosa of either noninfected or *H pylori*–infected patients at various stages of Correa's cascade. LATS2 and YAP1 were strongly up-regulated and nuclear in gastric epithelial cells of *H pylori*–infected patients compared with healthy mucosa, as early as the gastritis stage, characterized by the presence of lymphoid infiltrates (Figure 1*A*) and positive *H pylori* staining. LATS2 and YAP1 nuclear overexpression were found precisely within the isthmus in the fundus and in the crypts in the antrum, which corresponds to the location of

the regenerative epithelial progenitors, which are stimulated in response to *H pylori* infection for tissue regeneration.[9,19] LATS2 or YAP1 nuclear staining was even stronger in the glands composing the intestinal metaplasia lesions, in which the gastric mucosa is replaced by an epithelium showing intestinal morphology with the presence of mucous-secreting goblet-like cells (Figure 1A). LATS2 and YAP1 staining intensities on GC tissue sections were more heterogeneous than in nontumor tissues, with nuclear LATS2 directly correlating to nuclear YAP1 overexpression in intestinal-type GC (Figure 1A and B). Thus, LATS2 and YAP1 appeared concomitantly overexpressed and nuclear in gastric epithelial cells in *H pylori*–associated gastritis, intestinal metaplasia, and in GC.

The Correa cascade can be reproduced in a C57BL/6 mouse model force-fed with *Helicobacter felis* or with certain proinflammatory strains of *H pylori* such as the cytotoxin-associated gene A-pathogenicity island (cagPAI)- and *cagA*-positive *H pylori* HPARE strain (Figure 1C), as previously described.[9,19,20] The exception in these mouse models is that they do not develop a true intestinal metaplasia with goblet cells as in human beings, but a spasmolytic polypeptide expressing metaplasia composed of mucous-producing cells, replacing parietal and chief cells, and that can evolve after 1 year into pseudointestinal metaplasia composed of enterocyte-like cells characterized by an absorptive intestinal cell morphology in the upper portion of metaplastic glands.[9,19,20] In noninfected mouse stomachs, both LATS2- and YAP1-nuclear positive cells were restricted to the isthmus areas, as in human beings. An intense nuclear expression of LATS2 and YAP1 was noted in pseudointestinal-type metaplasia, but not in mucinous metaplasia. This LATS2 and YAP1 colabeling was even stronger in areas of dysplasia (Figure 1C).

The Hippo Pathway Genes Are Affected by H pylori

For further insight on the dynamics of LATS2 and YAP1 expressions triggered by *H pylori*, we used the human gastric epithelial AGS cell line as a model cell system of replicating gastric mucosa responding to *cagA*-positive *H pylori* strains by proinflammatory mediators and LATS2 up-regulation,[7] along with EMT.[8,9] Global gene expression of AGS in response to *H pylori* was performed at 24 hours using whole-genome microarrays. Genes involved in the Hippo pathway and whose expressions were altered significantly by the infection are presented in Figure 2A. The Hippo kinases MST1 and MST1R, but not LATS2 (previously reported to be posttranscriptionally up-regulated upon *H pylori* infection[7] and therefore not visible on the transcriptome), were up-regulated approximately twice upon infection, as well as YAP1, along with vestigial-like family member 4 (VGLL4), a YAP1-negative competitor for TEAD binding, which regulates its oncogenic function.[21] Other transcription factors speculated to be interacting with YAP1 were affected variably (TEADs, RUNX1, SMAD3). Several YAP1/TEAD target genes involved in cell proliferation and survival were affected significantly upon infection,

including conective tissue growth factor (CTGF) encoding a cysteine-rich extracellular matrix protein that functions as an integrin ligand and activates cell proliferation.[12]

The Hippo pathway upstream effectors and some components of cell polarity complexes and intercellular junctions, which contribute to the activation of the Hippo pathway,[21] were affected modestly upon infection, except the intercellular junction components CDH1 encoding E-cadherin, according to our previous report,[8] Crumbs Cell Polarity Complex Component 3 (CRB3) encoding a component of the Crumbs complex maintaining the epithelial integrity,[22] and AJUBA encoding a scaffold protein of cell junctions and binding partner of LATS2.[23]

Thus, analysis of the Hippo transcriptome in AGS upon infection combined with our previous report on LATS2[7] shows concomitant up-regulation of the core kinases, downstream effector genes, and the YAP1/TEAD target genes. A closely superimposable gene profile to that of *H pylori*–infected AGS cells relative to noninfected cells was obtained with another human gastric epithelial cell line, MKN74, which expresses a higher diversity of Hippo genes than AGS (Figure 2B and C).

Biphasic Kinetics of Hippo Activation Upon H pylori Infection of Gastric Epithelial Cells In Vitro

To assess how LATS2 and YAP1 are orchestrated during infection, we performed a time course analysis of their expressions in response to *H pylori* infection in AGS and MKN74 cell lines. To circumvent the limitations of the use of GC-derived cell lines, and because it is not possible to culture primary gastric epithelial cells in conventional adherent culture conditions, 2 nontumorigenic immortalized human epithelial cell lines also were used: the retinal pigment epithelial cells (RPE1) cell line, which is a good model to study the Hippo pathway,[24] and the human mammary epithelial cells (HMLE) cell line, which has been widely used to study EMT and the regulation of the Hippo/ YAP pathway.[25,26] The *cagA*-positive wild-type (WT) *H pylori* strain progressively triggered LATS2 and YAP1 accumulation in all cell lines after 2 hours of *H pylori* infection (HPI) and until 24 hours of HPI (Figure 3A). This was associated with an increase of LATS2-mediated YAP phosphorylation on Ser127 and of the ratio of YAP-phospho-Ser127 on total YAP (Figure 3B) and upstream to LATS2 phosphorylation on Thr1041 as shown for HMLE cells, altogether reflecting LATS2 activation between 2 and 24 hours of HPI. No changes were observed before 1 hour of HPI in HMLE cells (Figure 3A). Accordingly, LATS2 and YAP1 immunofluorescence analysis showed a progressively increasing number of brightly fluorescent cells, in which both were accumulated in the nucleus: although YAP1 nuclear accumulation seems maximal at 2 hours of HPI in all cell lines and then reduced at 24 hours of HPI, the nuclear accumulation of LATS2 appears progressively increased from 2 hours of HPI and up to 24 hours of HPI (Figure 3C and D). These changes in LATS2 and YAP protein expression (Figure 3A) and nuclear localization (Figure 3C and D) were not observed or strongly reduced at 2, 5, and 24 hours
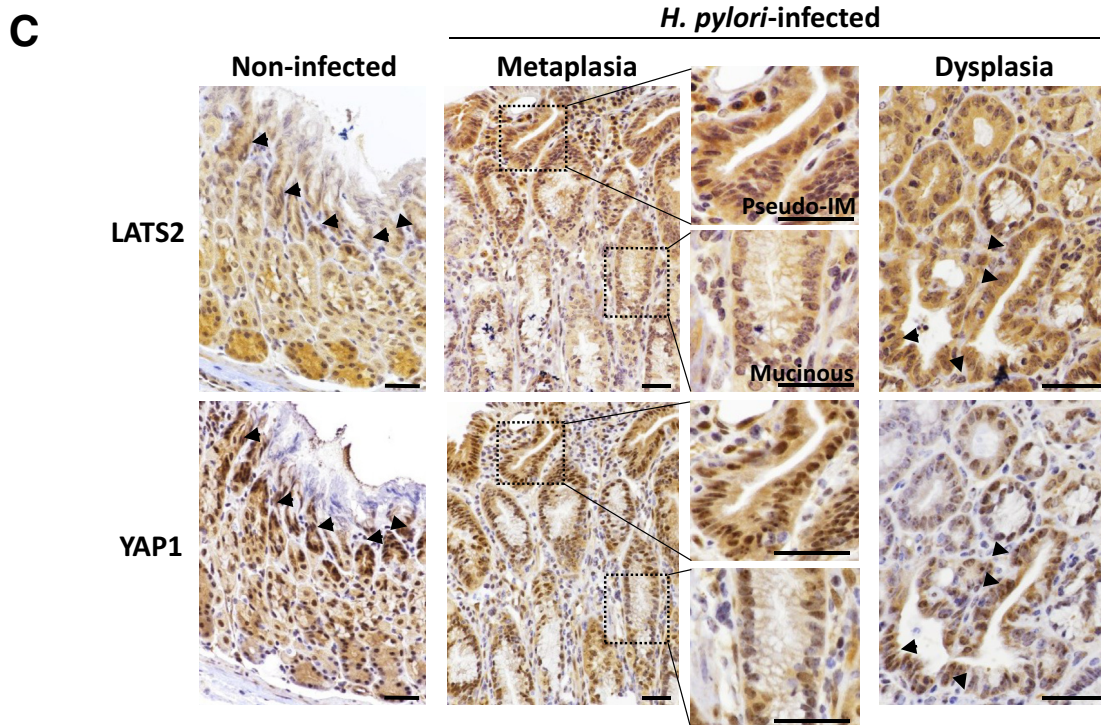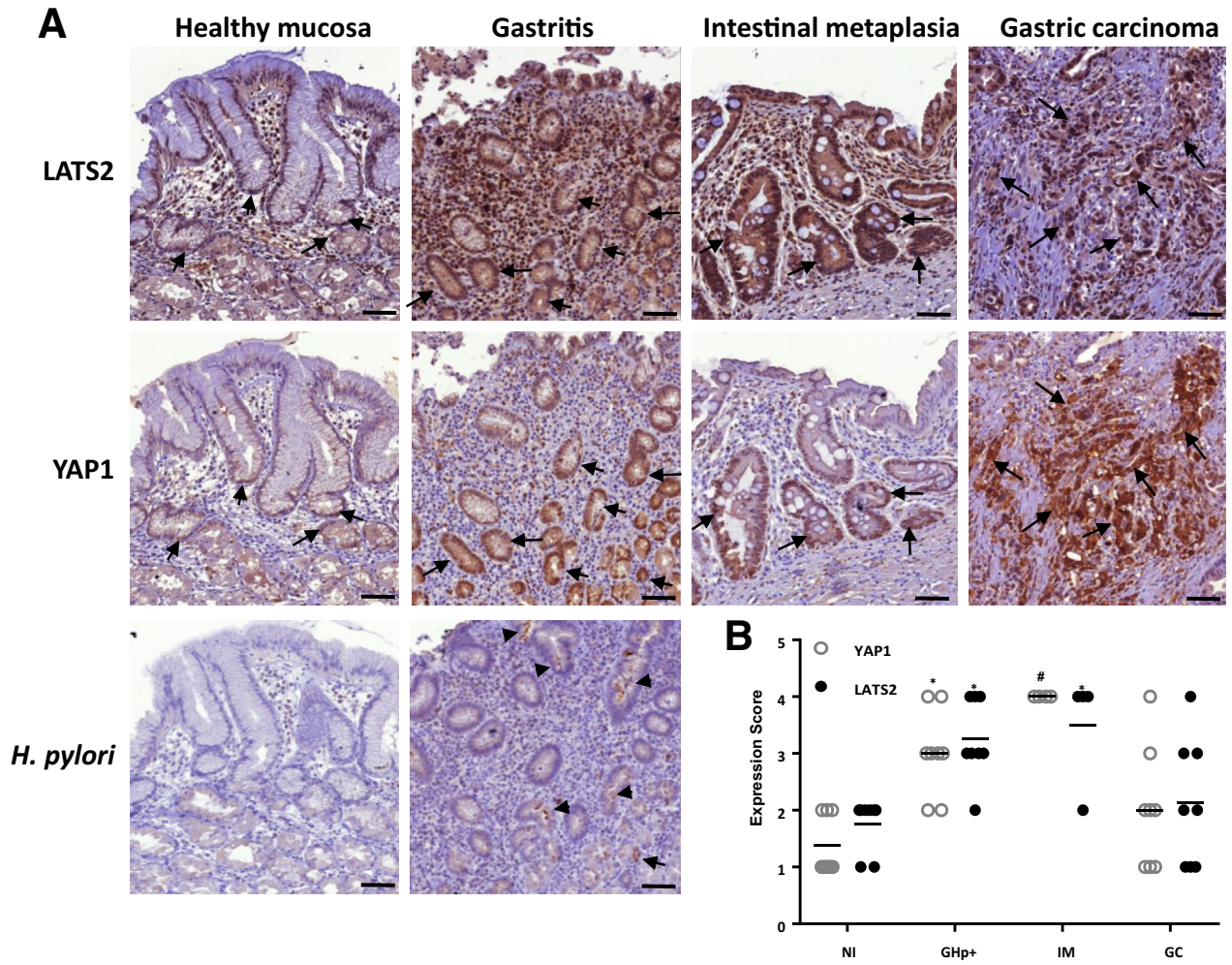
of HPI in cells infected with the *cagA*-deleted isogenic *H pylori* mutant (Δ*cagA*). These results were confirmed by reverse-transcription quantitative polymerase chain reaction (RT-qPCR) data in the 4 cell lines, with LATS2 and YAP1 messenger RNA (mRNA) overexpressed progressively upon infection with WT *H pylori*, but not with the Δ*cagA* mutant (Figure 4*A*). These results indicate that LATS2 and YAP1 overexpression and nuclear accumulations upon infection mostly require the virulence factor CagA (Figures 3*A–D* and 4*A*). The variations in LATS2 protein being more important than those in mRNAs are concordant with a posttranscriptional regulatory mechanism previously described in the AGS gastric cell line.[7]

Because TEAD is considered to be the primary transcriptional partner of YAP1, we used a TEAD-luciferase reporter assay to sense YAP1/TEAD-mediated transcription in AGS and MKN74 cells challenged by *H pylori* (Figure 4*B*). TEAD transcriptional activity showed biphasic kinetics characterized by an early and transient stimulation during the first 2 hours of HPI, followed by decreasing activity from 5 to 24 hours of HPI with WT *H pylori*. These observations are in agreement with the YAP1 nuclear accumulation that appeared maximal at 2 hours of HPI in AGS and MKN74 cells (Figure 3*C* and *D*). The activation of TEAD-luciferase activity at 2 hours of HPI and its inhibition at 24 hours of HPI are dependent on CagA because they were not observed in both AGS and MKN74 cells challenged with the Δ*cagA* mutant (Figure 4*B*). The changes in the expressions of CTGF and CYR61, the 2 main YAP1/TEAD target genes,[12] paralleled those of TEAD-luciferase activity with an activation at 2 hours of HPI in AGS, MKN74, and RPE1 cells (Figure 4*C*), and repression at 24 hours of HPI in AGS, RPE1, and HMLE cells (except in MKN74 cells, in which their expression remained increased at 24 hours of HPI). This was observed in response to the WT strain but not in response to the Δ*cagA* mutant strain. These results indicate that *H pylori* transiently triggered YAP1/TEAD-mediated transcription, and then progressively repressed it by activating the Hippo pathway kinase LATS2. It is noteworthy that the activation of the Hippo/YAP1/TEAD pathway was CagA-dependent (Figure 4*B* and *C*).

At a functional point of view, the Hippo pathway restricts cell proliferation.[11] Indeed, the growth rate of *H pylori* 7.13 WT-infected AGS at 24 hours of HPI assessed by cell numeration was reduced by 73.5% ± 8.0% (n = 4)

compared with noninfected cells, conforming to our previous report on *cagA*+ *H pylori* strains inducing a cell-cycle arrest in AGS cells at the G1/S transition.[7] Similar growth inhibition also was observed in *H pylori* 7.13 WT-infected MKN74 cells (by 42.5% ± 8.4% at 24 hours of HPI and 64.2% ± 7.5% at 48 hours of HPI, n = 3) compared with noninfected ones. Down-regulation of the S-phase marker proliferating cells nuclear antigen (PCNA) at 24 hours of HPI with *H pylori* 7.13 WT in AGS (reduced to 33.07% ± 10.75%) and MKN74 cells (reduced to 74.04% ± 12.93%) compared with noninfected ones corroborated the infection-induced growth inhibition.

Altogether these data show that *H pylori* transiently triggered YAP1 expression and activation and YAP1/TEAD transcriptional activity at 2 hours of HPI, while progressively promoting the accumulation of LATS2, which, phosphorylating YAP1 on Ser127, targeted it for proteasomal degradation and hence inhibited the TEAD-mediated transcriptional activity from 5 to 24 hours of HPI, eventually contributing to the cell growth inhibition observed in response to *H pylori* infection.

LATS2 and YAP1 Positively Regulate Each Other's Expression in Basal Conditions and in Response to H pylori

To further assess how LATS2 and YAP1 are regulated in response to *H pylori*, we modulated their respective expression using specific small interfering RNAs or expression vectors. As expected, siLATS2 successfully knocked down LATS2 expression and siYAP1 knocked down YAP1 expression in basal conditions and they prevented their respective overexpression induced at 24 hours of HPI with *H pylori*, at both protein and mRNA levels in AGS, MKN74, and RPE1 cells (Figure 5*A* and *C*). LATS2 silencing also markedly decreased LATS2-mediated YAP1-P^{Ser127} accumulation compared with small interference RNA Control (siControl) cells (Figure 5*A*), and increased the YAP/TEAD-mediated TEAD transcriptional activity (Figure 5*D*). Conversely, transfecting a constitutively active LATS2 expression vector[7] inhibited TEAD transcriptional activity by 70% compared with a control vector (plasmid Enhanced Green Fluorescent Protein, pEGFP), while transfecting vectors encoding either the WT YAP1 (plasmid YAP1, pYAP1) or a constitutively active, non-phosphorylatable, YAP1^{S127A}

Figure 1. (*See previous page***). LATS2 and YAP1 expressions in *H pylori*–infected (*A* and *B*) human and (*C*) mouse gastric mucosa.** (*A*) Representative images of the immunohistochemistry staining (dark brown) of LATS2 and YAP1 in the gastric mucosa of noninfected individuals (healthy mucosa), with *H pylori*–associated gastritis, intestinal metaplasia, or GC. *Black arrows* indicate nuclear expression of both LATS2 and YAP1 in the isthmus region of the noninfected mucosa and notably in gastritis, intestinal metaplasia, and gastric carcinoma cells. *Arrowheads* indicate *H pylori* detection in the lumen of the glands (brown staining). *Scale bars*: 100 μm. (*B*) Scores of the relative percentages of LATS2 and nuclear YAP1-positive cells determined for *H pylori* negative (n = 7) and *H pylori*–positive patients with gastritis (GHp+, n = 7), intestinal metaplasia (IM, n = 4), or GC (n = 7), from the experiments shown in panel *A*. The difference between the groups was evaluated using the Fisher exact test. *P < .05, #*P* < .01. (*C*) Representative LATS2 and YAP1 staining on gastric tissue sections from noninfected C57BL/6 mice and at various stages of the transformation cascade of the gastric mucosa upon infection with *H pylori* HPARE strain. *Arrowheads* indicate intense nuclear expression of both LATS2 and YAP1 in the isthmus region of the noninfected mucosa and notably in pseudointestinal-like metaplasia (pseudo-IM, *enlarged box*) and dysplasia observed after 12 months. LATS2 and YAP1 expression was not increased in mucinous metaplasia. *Scale bars*: 50 μm. NI, non-infected.

mutant (pYAPS127A) stimulated TEAD activity by 3- and 6-fold, respectively, in AGS cells, with similar results in MKN74 cells (Figure 5D). Although YAP1 silencing prevented *H pylori*–induced activation of TEAD transcriptional activity at 2 hours of HPI, LATS2 silencing prevented *H pylori*–induced inhibition of TEAD transcriptional activity

A

B

C
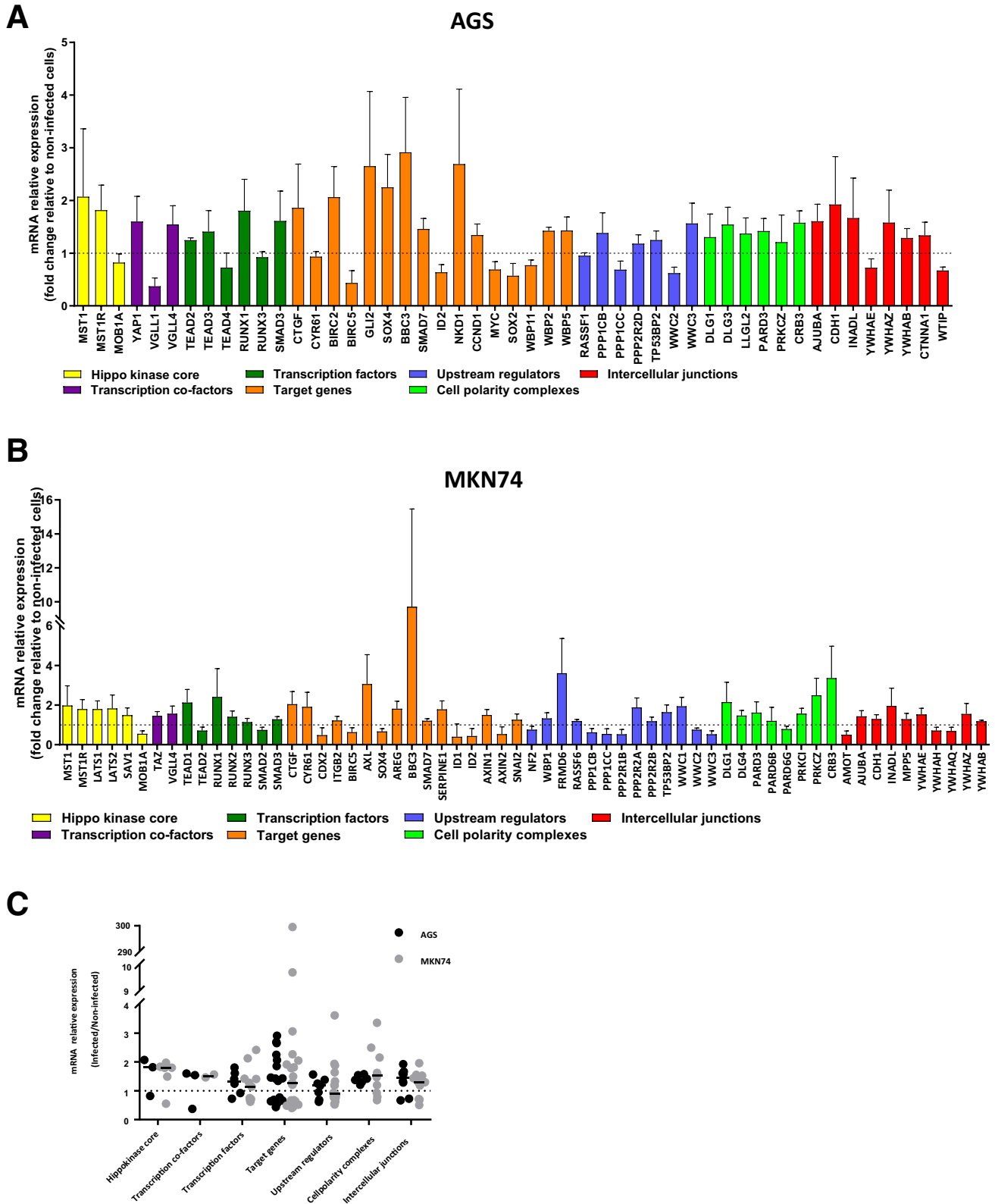
at 24 hours of HPI, resulting in an increase of the expression of CTGF and CYR61 YAP/TEAD target genes in AGS, MKN74, and RPE1 cells at 24 hours of HPI (Figure 5*E* and *F*). Unexpectedly, LATS2 silencing also decreased YAP1 expression in basal conditions (Figure 5*A*) and prevented *H pylori*–induced YAP1 overexpression at 24 hours of HPI at the protein and/or mRNA levels in AGS, MKN74, and RPE1 cells (Figure 5*A* and *C*). Reciprocally, YAP1 silencing down-regulated LATS2 expression at the protein and/or mRNA levels in AGS, MKN74, and RPE1 cells (Figure 5*A* and *C*). These results suggest that in basal conditions LATS2, similar to CTGF and CYR61, may depend on YAP1/TEAD transcriptional activity. Collectively, these data confirm on one hand the canonical function of YAP1 as a mandatory TEAD transcription cofactor in these models, and on the other hand they stress an unexpected correlation of LATS2 and YAP1 expressions beyond their kinase-substrate relationship.

All combined, these data show that in basal conditions as well as in response to *H pylori*, (1) YAP1 is a major coactivator of TEAD-mediated transcription at 2 hours of HPI, (2) that it is prominently controlled by LATS2-mediated YAP1 phosphorylation and targeting for degradation at 24 hours of HPI, and, remarkably, (3) that LATS2 and YAP1 reciprocally positively regulate each other's expression. This last conclusion was supported further by data on other gastric epithelial cell lines, which show a strict co-expression of YAP1 and LATS2 (Figure 5*B*).

### LATS2 Restricts the H pylori–Induced EMT

We observed that either YAP1 or, to a lesser extent, LATS2 silencing hampered the AGS and RPE1 growth rate in basal conditions (reduced by 41% ± 5% [$P < .05$ vs respective siControl cells] with siYAP1 and 30% ± 12% [$P < .05$ vs respective siControl cells] with siLATS2 compared with siControl at 30 hours in AGS cells, and by 39% ± 8% [$P < .05$ vs respective siControl cells] with siYAP1 and 6% ± 15% with siLATS2 compared with siControl at 30 hours in RPE1 cells). This suggests that the LATS2/YAP1 tandem may be required for optimal cell growth in tissue culture. Moreover, we noticed in AGS that some siLATS2 cells acquired the EMT-characteristic hummingbird phenotype, and that siLATS2 significantly increased the percentage of hummingbird cells induced by *H pylori* at 24 hours of HPI (Figure 6*A* and *B*). Similar results were observed in MKN74, in which the rounded cells undergoing EMT (as previously described[8]) was increased in siLATS2 cells compared with siControl cells (Figure 6*A*). The mesenchymal phenotype observed in siLATS2-treated cells was associated with ZEB1

up-regulation and nuclear accumulation compared with siControl, in both basal and infected conditions in AGS, MKN74, and RPE1 cells (Figure 6*C* and *D*). Noticeably, LATS2 silencing also drastically up-regulated other mesenchymal effectors such as the matrix metalloproteinase-9 (MMP9) and the bone morphogenic protein-1 (BMP1) (Figure 6*C* and *E*). Exacerbated EMT upon LATS2 silencing was confirmed by increased invasive properties in both basal and *H pylori*–infected conditions compared with siControl in AGS and MKN74 cells and in basal conditions in RPE1 cells (Figure 6*F*). On the contrary, exogenous plasmid-LATS2 (pLATS2) slowed down basal AGS invasive capacities (Figure 6*F*). Collectively these results support a role of LATS2 in contributing to the basal epithelial phenotype in gastric epithelial cell lines as well as in RPE1 epithelial cells and in constraining *H pylori*–promoted EMT.

LATS2 Controls the H pylori–Induced Metaplasia Phenotype

Next, we analyzed the changes in expression of highly specific markers of intestinal metaplasia in gastric AGS and MKN74 cells. The expression of the caudal-type homeobox protein 2 (CDX2), mucin 2 (MUC2), and intestinal alkaline phosphatase (IAP) was evaluated in siControl and siLATS2 AGS cells challenged by WT *H pylori*. CDX2 is a critical actor in the development of intestinal metaplasia.[27] As an intestine-specific transcription factor, CDX2 regulates goblet-specific MUC2 gene expression, resulting in the differentiation of intestinal epithelium.[28] IAP, a brush-border protein expressed exclusively in differentiated enterocytes, is a host defense mechanism preventing bacterial invasion across the gut mucosal barrier.[29] AGS cells heterogeneously expressed CDX2 detected by immunofluorescence in the nucleus in basal conditions (Figure 7*A* and *C*). The percentage of CDX2-positive cells increased by more than 2-fold in response to infection in siControl cells, and by more than 5-fold and 6.5-fold in noninfected and infected, respectively, siLATS2 cells (Figure 7*A* and *C*). Accordingly, CDX2 mRNA was up-regulated in infected siControl cells, as well as in both noninfected and infected siLATS2 AGS cells, compared with noninfected siControl cells (Figure 7*D*). However, CDX2 upregulation could not be confirmed in siLATS2 MKN74 cells (Figure 7*E*). MUC2 immunofluorescent staining was heterogeneous and mostly nuclear in noninfected siControl cells, as previously reported in AGS cells,[30] and its overexpression in siLATS2 cells in basal and infection conditions paralleled those of CDX2 both at the protein and the mRNA level in AGS cells (Figure 7*A*

Figure 2. (*See previous page*). **Expression of the Hippo pathway genes upon 24 hours of *H pylori* infection of cultured human gastric epithelial cells.** (*A* and *B*) Microarray-based identification of differentially expressed Hippo pathway–associated genes in response to *H pylori* 7.13 WT infection in (*A*) AGS cells and (*B*) MKN74 cells. Hippo kinase core genes correspond to *yellow bars*, transcriptional co-factors to *purple bars*, YAP1/TAZ/TEAD target genes to *orange bars*, Hippo upstream effectors to *blue bars*, components of the cell polarity complexes to *light green bars*, and intercellular junctions to *red bars*. (*C*) Relative expression of the differentially expressed Hippo-related genes in response to *H pylori* infection in AGS and MKN74 gastric epithelial cell lines was determined according to microarray-based transcriptome analyses. *Bars* indicate medians. (*A–C*) Only genes with statistically significant changes in expression are shown (n = 4; $P < .05$ in *t* test with Benjamini–Hochberg correction). LATS2 was not expressed differentially in AGS cells upon infection.
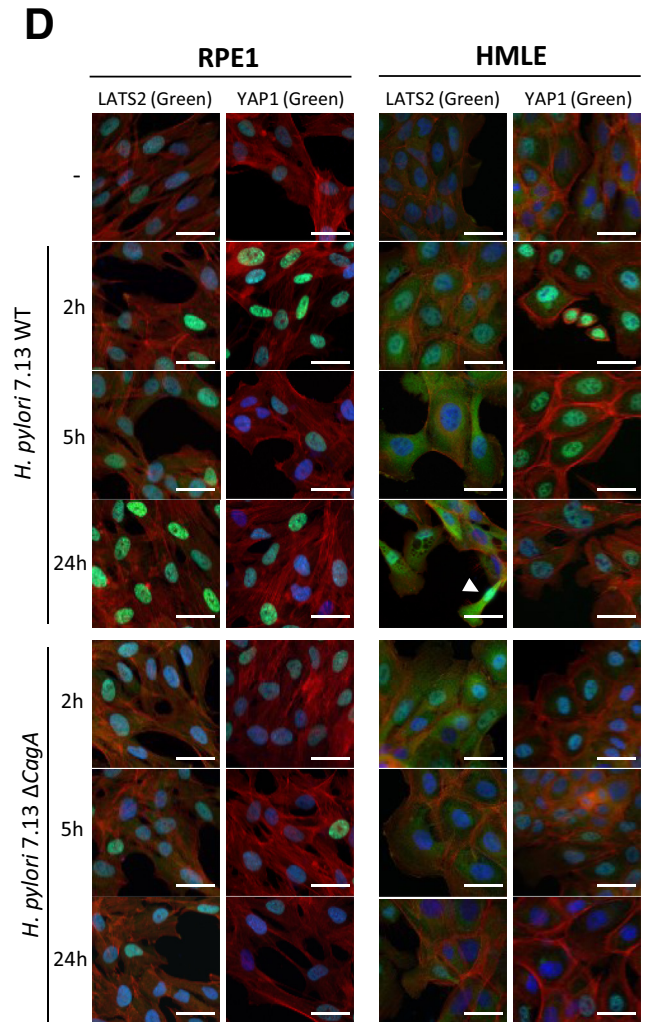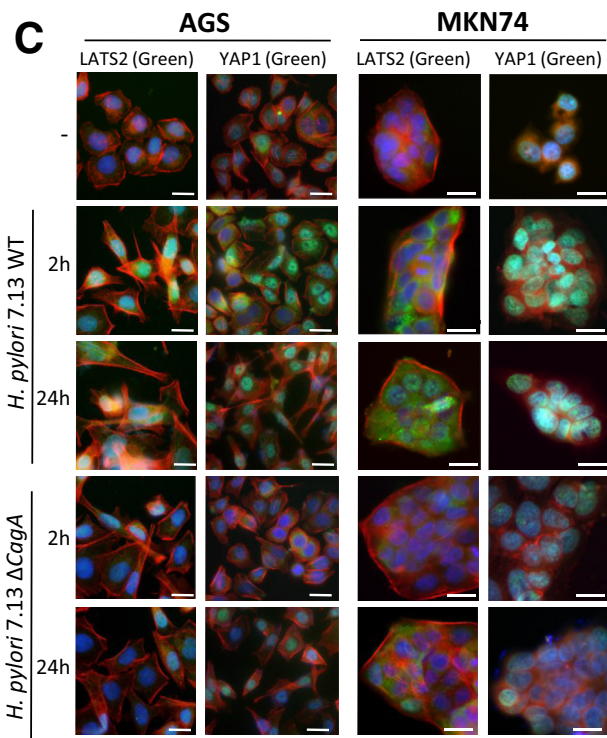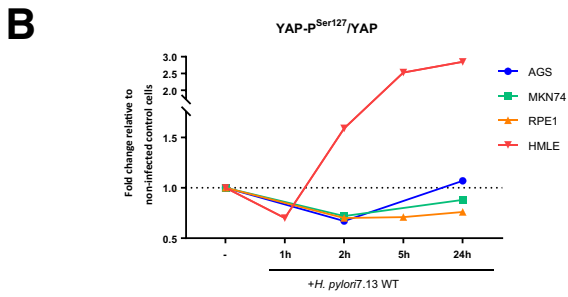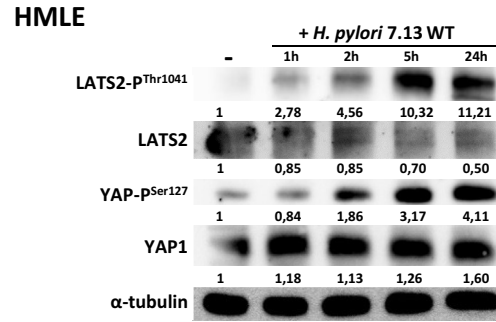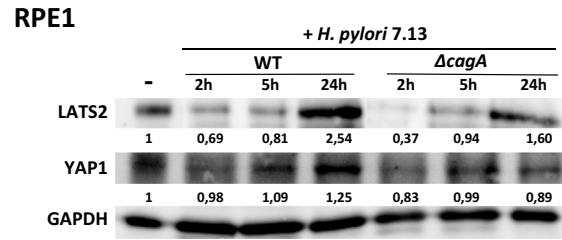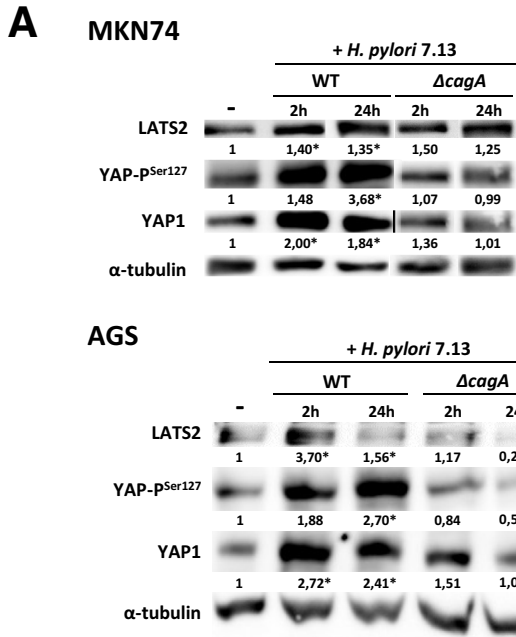
and *D*). IAP enzymatic activity appeared as cytoplasmic blue foci in AGS cells; the percentage of cells showing IAP foci was increased upon infection and particularly in siLATS2 infected cells, along with larger and more intense foci (Figure 7*B* and *C*).

Other intestinal metaplasia markers such as keratin 7 (KRT7) and Sox9 transcription factor have been reported to be associated with *H pylori*–induced metaplasia,[31] and KRT7 also was found to be up-regulated in response to *H pylori* and to LATS2 silencing in AGS (Figure 7*D*). Thus, the significant overexpression of MUC2, CDX2, IAP, and KRT7 in siLATS2 infected AGS cells compared with siControl infected cells confirms that LATS2 silencing exacerbated *H pylori*–induced expression of markers of intestinal metaplasia in this particular cell line. As far as MKN74 cells are concerned, in which LATS2 silencing did not affect CDX2 expression but clearly up-regulated Sox9 (Figure 7*E*), the gastric-specific mucin-5AC (MUC5AC), which is well expressed in MKN74 cells but not in AGS cells (data not shown), was down-regulated in MKN74 cells upon infection and further decreased in infected or noninfected siLATS2 cells (Figure 7*E*), signifying a loss of gastric epithelial differentiation markers.

All combined, these data indicate that LATS2, while controlling *H pylori*–promoted EMT, also constrains the intestinal transdifferentiation endorsed by the infected gastric epithelial cells.

Discussion

Epithelia exposed to environmental assaults, including pathogen infection, require constant cell renewal and signaling tuning to maintain tissue homeostasis. Upon contact and molecular communication with its host, mainly through the *cag*PAI-encoded effectors, *H pylori* manipulates host signaling cascades. This occurs by either modulating or hijacking specific intracellular signal transduction components, thereby undermining host defenses and establishing chronic infection and gastric diseases at high oncogenic risk. The Hippo pathway, an evolutionary conserved signaling cascade regulating tissue growth and homeostasis through the downstream core kinase/effector tandem constituted by LATS1/2 and YAP1, is not fully understood in *H pylori* infection. We previously reported that carcinogenic strains of *H pylori* up-regulated the tumor-suppressor LATS2,[7] and increased EMT features[8,9] in gastric epithelial cells. The role

of LATS2 and its oncogenic target YAP1 remain to be clarified during the preneoplastic steps of *H pylori*–induced gastric carcinogenesis, including metaplasia development. Our data show that the Hippo pathway is an additional signaling cascade triggered in host cells in response to *H pylori* in a CagA-dependent manner. Moreover, they stress a prominent role of LATS2 in allowing the host cells to resist the *H pylori*–mediated transdifferentiation of the gastric epithelium, characterized by the acquisition of both EMT and intestinal metaplasia markers.

LATS2 and YAP1 Interdependence in H pylori–*Infected Gastric Mucosa*

In our study, we found LATS2 and YAP1 concomitantly up-regulated in the nuclei of the epithelial cells in the gastric mucosa of both patients and mice chronically infected with *H pylori*, as soon as the gastritis stage and increasingly in the preneoplastic lesions of intestinal metaplasia preceding adenocarcinoma development. They both were strongly, still heterogeneously, expressed in intestinal-type GC. These observations were unexpected in regard to most data reporting an inverse correlation of LATS1/2 and YAP1 expressions in many tumor cells.[11,14] The overexpression of the oncogenic YAP1 was reported to portend a poor prognosis in GC.[15–17] YAP1 is strikingly essential to stimulate cell growth when they are stirred up to ensure tissue regeneration,[32–35] a condition fulfilled during *H pylori* assault of the gastric mucosa. In turn, LATS2 acts as a brake of the stimulated growth, phosphorylating and targeting YAP1 for proteasomal degradation and thereby ensuring optimal organ size. By using AGS and MKN74 gastric epithelial cell lines as well as HMLE and RPE1, 2 nongastric immortalized epithelial cell lines, challenged by *H pylori* in vitro, we found that *H pylori* via CagA affects LATS2 and YAP1 expression and activity in a coordinated biphasic pattern, characterized by the following: (1) by an early and transient YAP1 nuclear accumulation along with stimulated YAP1/TEAD transcription at 2 hours of HPI, (2) followed by nuclear LATS2 up-regulation leading progressively to YAP1 phosphorylation from 2 to 24 hours of HPI, (3) which correlated with a progressive decrease and repression at 24 hours of HPI of TEAD transcriptional activity and expression of CYR61 and CTGF target genes. In vitro, this quick wave of YAP1/TEAD activation may be rapidly

Figure 3. (*See previous page*). **Expression and subcellular localizations of *H pylori*–induced changes in LATS2 and YAP1 expressions in cultured gastric and nongastric cells.** Time course analyses were performed in gastric AGS and MKN74 and in nongastric noncancerous epithelial cells (HMLE and RPE1) infected with the *H pylori* 7.13 WT strain and the *cagA*-deleted isogenic mutant (Δ*cagA*) strain for different time periods during 24 hours. (*A*) LATS2, LATS2-P^{Thr1041}, total YAP1, and YAP-P^{Ser127} protein levels were analyzed by Western blot in noninfected cells, at the indicated time periods during 24 hours of HPI with WT *H pylori* and at 24 hours of HPI with the *cagA*-deleted isogenic mutant. A representative blot of 3 or more experiments is shown. The number under each *band* corresponds to the value of the relative protein quantification normalized to the housekeeping protein (glyceraldehyde-3-phosphate dehydrogenase [GAPDH] or α-tubulin). *$P < .05$ vs noninfected AGS or MKN74 cells. (*B*) Graphic representation of the ratio of YAP-P^{Ser127} on total YAP1 during kinetics of infection of *H pylori* 7.13 WT in the 4 cell lines. (*C* and *D*) Representative images of the expression and subcellular localization of LATS2 and YAP1 (in green) evaluated by immunofluorescence in (*C*) AGS and MKN74 gastric epithelial cells at 2 and 24 hours of HPI, and (*D*) in RPE1 and HMLE nongastric noncancerous epithelial cell lines at 2, 5, and 24 hours of HPI. Actin was marked with phalloidin–Alexa Fluor–546 (in red) and nuclei were marked with 4'-6-diamino-phenyl-indol (in blue). *Scale bars*: 10 μm.
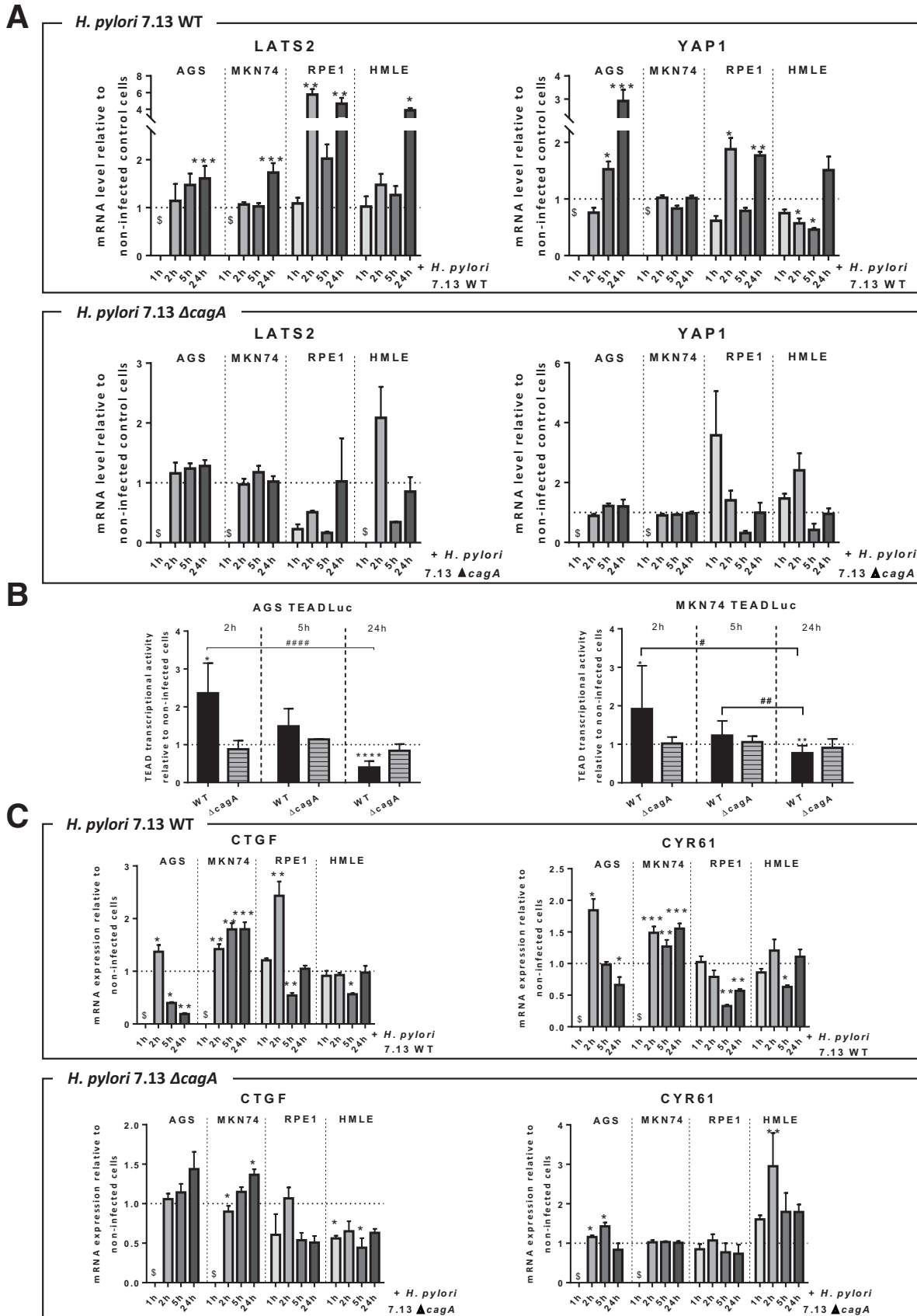
controlled by LATS2 induction in response to *H pylori*. Unlike LATS2, LATS1 could not be detected by RT-qPCR in AGS and MKN74 cell lines (unpublished data), suggesting that LATS1 probably plays a minor role in the response to *H pylori*, contrarily to LATS2. In addition, Furth and Aylon[36] reported that although LATS1 protein is detected throughout most tissues, LATS2 protein levels seem to vary, with the highest expression in the gastrointestinal tract and the brain. In vivo, chronic infection and inflammation of the gastric mucosa by *H pylori* could lead to constant waves of YAP1/TEAD activation and LATS2 induction that may result in the observed YAP1–LATS2 nuclear co-overexpression, preceding neoplastic transformation and maintained in the growing GC. Interestingly, LATS2 and YAP1 overexpression in nontumor tissues were found precisely within the isthmus of the fundus and in the crypts of the antrum, where the stem cell marker CD44 also was overexpressed, and that corresponds to the regenerative epithelial stem cell location.[18] This co-overexpression may show an extension of the gastric stem cell reservoir, which, in the context of *H pylori*–triggered chronic inflammation, acquires mesenchymal, intestinal, and preneoplastic features.

The siLATS2- and siYAP1-mediated loss-of-function experiments showed that knocking down one weakens the expression of the other, suggesting that LATS2 and YAP1 reciprocally maintain each other's expression and activity in both basal and infected conditions. Moroishi et al[37] reported that YAP1/TEAD directly induces LATS2 transcription upon binding to its promoter. LATS2 in turn phosphorylates YAP1 on Ser[127], leading to its targeting for proteasomal degradation: this negative feedback loop likely is responsible for the transient and tightly controlled YAP1/TEAD activation in *H pylori*–challenged gastric and nongastric epithelial cells in vitro, despite the overexpression of YAP1 and its nuclear localization at 24 hours of HPI. For instance, nuclear YAP1 also can associate with repressors such as VGLL4,[24] RUNX1, and RUNX3,[38,39] which by binding YAP1 inhibit its association with the TEADs and the subsequent TEAD-mediated transcriptional activity. Interestingly, VGLL4 and RUNX1 were found twofold increased in the transcriptome of AGS and MKN74 cells at 24 hours of HPI (Figure 2). Therefore, it cannot be excluded that the overexpression of these negative regulators of YAP1/TEAD interaction also could participate in the observed effects at 24 hours of HPI.

The YAP1/TEAD-dependent transcription of LATS2 also is supported by the strong correlation of LATS2 and YAP1 protein in other gastric epithelial cell lines. Therefore, LATS2 could be considered a YAP1 target gene involved in a negative feedback loop to tightly control YAP1/TEAD oncogenic activity while partly maintaining YAP1 expression. The LATS2/YAP1 interdependence also could explain the impaired cell growth in siLATS2 AGS cells, contrarily to enhanced growth that could be expected after knockdown of a tumor-suppressor gene.

At last, one open question is how LATS2 and YAP1 are alerted by *H pylori* infection. In addition to MST1/2, which was up-regulated 2-fold in AGS and MKN74 cells (transcriptomic analyses) (Figure 2) and induces LATS2 phosphorylation on Thr1041 and its subsequent activation (Figures 3 and 5), LATS2 is subject to regulation by numerous proteins, including Mitogen-associated protein kinase 4 (MAPK4), AURORA-A, and AJUBA, Neurofibromatosis 2 (NF2)/Merlin, and CRB3,[11,40–42] which were found to be up-regulated in the transcriptome of infected gastric epithelial cells (Figure 2). Moreover, mechanical signals related to the microenvironment represent an additional pillar for YAP1 function.[12,34,43] CagA, through its ability to bind to several host cell junction proteins, deeply destabilizes gastric epithelial cell–cell junctions and cell shape, as evidenced by the hummingbird phenotype that AGS show at 24 hours of HPI.[8,9,44–46] It is noteworthy that CagA targets and triggers the Src-homology phosphatase-2 (SHP-2), which directly interacts with YAP1 and potentiates its cotranscriptional function.[47,48] This tripartite connection of CagA/SHP2/YAP1 may be critical in the early phases of human gastric carcinogenesis.[49] Nuclear localization of YAP1 is thus the sum of multiple, possibly parallel, regulatory layers.

LATS2 Constrains EMT and Intestinal Metaplasia in Infected Gastric Epithelial Cells

The oncogenic cascade leading to gastric carcinoma in chronically *H pylori*–infected gastric mucosa involves a transdifferentiation process termed the *intestinal metaplasia*, in which the gastric mucosa aberrantly differentiates into an intestinal mucosa, both morphologically and functionally.[1,4] We previously reported that this aberrant differentiation generated by the *H pylori*–mediated inflammatory context starts by the loss of epithelial features at the profit of mesenchymal ones, although the mucosa exacerbated some epithelial features (namely, the micro RNA miR-200 and E-cadherin expressions), which allowed it to thwart the irreversible loss of epithelial identity and resist total allostasis.[8]

LATS2 silencing increased YAP1/TEAD-mediated the oncogenic transcriptional program (objectified here by CTGF and CYR61 up-regulation under basal and *H pylori*–infected conditions) and exacerbated the *H*

Figure 4. (*See previous page*). **Biphasic kinetics of *H pylori*–induced changes in LATS2 and YAP1 expressions in cultured gastric and nongastric cells.** (*A*) Relative mRNA levels for LATS2 and YAP1 assessed by RT-qPCR at 1, 2, 5, and 24 hours of HPI with *H pylori* 7.13 WT and Δ*cagA* strains in AGS, MKN74, RPE1, and HMLE cell lines. (*B*) Biphasic kinetics of TEAD-luciferase reporter activity with *H pylori* 7.13 WT and Δ*cagA* at 2, 5, and 24 hours of HPI. (*C*) Relative mRNA levels for the YAP1/TEAD target genes CTGF and CYR61, assessed by RT-qPCR, in kinetics of infection with *H pylori* 7.13 WT and Δ*cagA* strains. (*A–C*) *Bars* represent means ± SEM of fold changes relative to noninfected cells, 3 < n < 6. *P < .05, **P < .01, and ***P < .001 vs noninfected, using the Kruskal–Wallis test. $^{$}$Unavailable data.
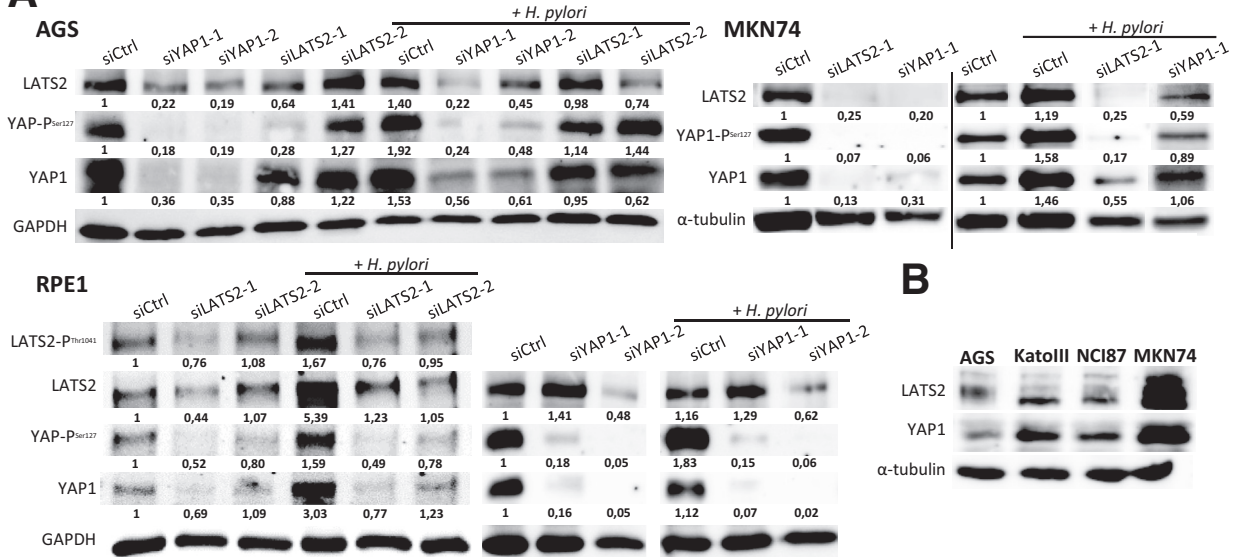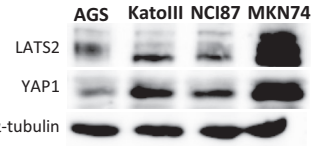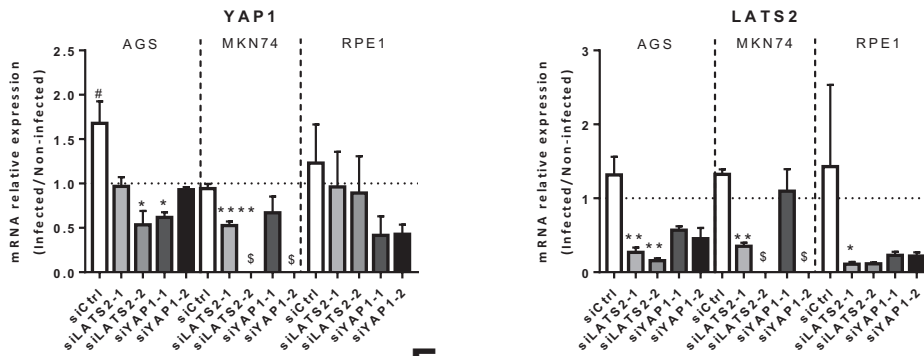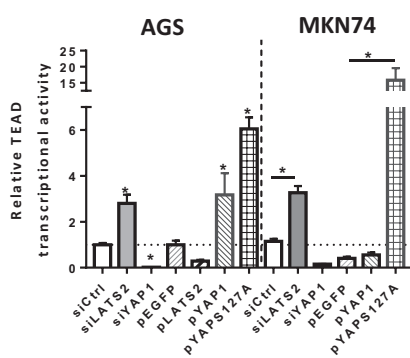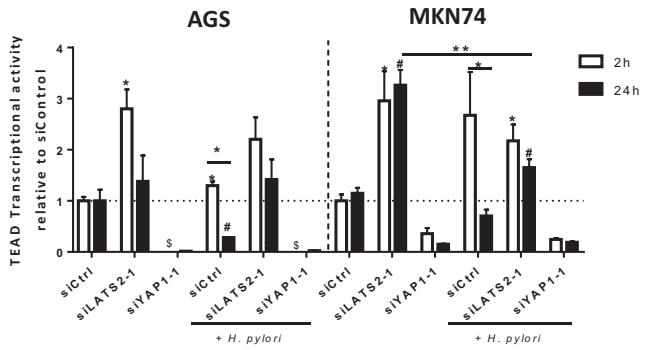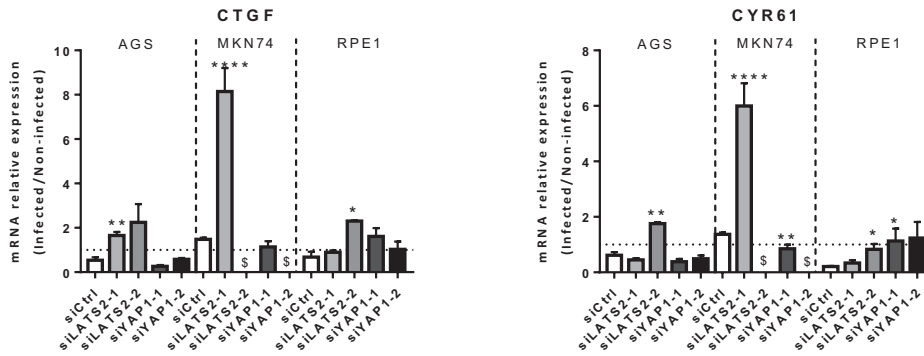
pylori–induced EMT phenotype, as shown by characteristic alterations in cell morphology, induction of the mesenchymal marker ZEB1, and the proteinases MMP9 and BMP1, which likely may be involved in the increased invasion capacities. Interestingly, ZEB1 mechanistically and functionally binds to YAP1, promoting the expression of a common ZEB1/YAP1 target oncogene set, including CTGF and CYR61,[50] the up-regulation of which in siLATS2 AGS cells could be mediated not only by YAP1/TEAD, but also by YAP1/ZEB1 as well. ZEB1 is also a NF-κB target gene during *H pylori*–induced EMT in gastric epithelial cell lines.[8] ZEB1 up-regulation, induced by siLATS2, could be explained by an indirect action of LATS2 via NF-κB, which was found to be regulated negatively by LATS2 in non–small-cell lung carcinoma.[51] In addition, silencing LATS2 in nontransformed HMLE mammary epithelial cells increased NF-κB association with p53, thereby promoting cell migration.[52]

Similar to EMT, intestinal metaplasia is an aberrant differentiation that can be partly mimicked in the cultured gastric cell system challenged by WT *H pylori*, as shown by the up-regulation of the intestinal metaplasia markers CDX2, MUC2, IAP, and KRT7 in AGS cells and up-regulation of the intestinal metaplasia marker SOX9 and down-regulation of the gastric-specific MUC5AC in MKN74 cells. CDX2 may be stimulated by interleukin 6 via the signal transducer and activator of transcription 3 pathway[53] and also by some mesenchymal effectors such as BMP1,[54] which was shown here to be up-regulated upon infection and upon LATS2 silencing in both AGS and MKN74 cells.

In conclusion, during the time course of *H pylori* infection, which interrupts the integrity of the gastric mucosa and provides access to its oncogenic effector CagA to many host cell signaling components, a number of specific signal transmissions are engaged through the different cell compartments.[55] The tumor-suppressor Hippo LATS2/YAP1/TEAD signaling is one of them: the co-overexpression of nuclear LATS2 and YAP1 detected in *H pylori*–associated gastritis and metaplastic tissues suggests that an equilibrium exists in vivo between active YAP1 and LATS2-mediated YAP1 targeting for degradation that could maintain gastric epithelial cell differentiation

and survival in the infected and inflamed mucosa. In the host–pathogen conflict, which generates an inflammatory environment, cell damage, and perturbation of epithelial turnover and differentiation, it appears as a protective pathway limiting the loss of gastric epithelial identity that precedes adenocarcinoma development. This manipulation also may be beneficial to *H pylori* colonization and chronic infection.

Materials and Methods

Ethic Statements on Human and Mouse Tissue Samples

Studies on paraffin-embedded tumors and distant nontumor tissues from gastric adenocarcinoma patients were performed in agreement with the Direction for Clinical Research and the Tumor and Cell Bank of the University Hospital Center of Bordeaux (Haut-Leveque Hospital, Pessac, France) and were declared at the French Ministry of Research (DC-2008-412). Animal experiments have been performed in level 2 animal facilities of the University of Bordeaux (France), with the approval of institutional guidelines determined by the local Ethical Committee of the University of Bordeaux and in conformity with the French Ministry of Agriculture Guidelines on Animal Care and the French Committee of Genetic Engineering (approval number 4608).

Human Gastric Tissues

Paraffin-embedded gastric tissue samples (tumors and noncancerous mucosa) from consenting patients (both sexes; age, 68–85 y) undergoing gastrectomy for distant noncardia adenocarcinoma were included in the study, in agreement with the tumor bank of the Bordeaux University Hospital (France), as previously reported.[17]

Gastric and Nongastric Epithelial Cell Culture

The AGS (ATCC CRL-1739), MKN74 (HSRR Bank JCRB0255), NCI-N87 (ATCC CRL-5822) and Kato-III (ATCC HTB-103) cell lines established from human GC were cultured in Dulbecco's modified Eagle medium/ F12-Glutamax or RPMI1640-Glutamax media for MKN74,

Figure 5. (*See previous page*). **LATS2 and YAP1 regulate each other both in basal conditions and in response to *H pylori* infection.** (*A*) Western blot analysis of LATS2, LATS2-P^{Thr1041}, YAP1, and YAP-P^{Ser127} protein levels in AGS, MKN74, and RPE1 cells infected or not with the 7.13 WT *H pylori* (24 hours of HPI) 30 hours after the last transfection with small interfering RNAs, either negative control (siCtrl), or against LATS2 (siLATS2-1 and siLATS2-2) or YAP1 (siYAP1-1 and YAP1-2). The numbers under each *band* correspond to the quantification of the relative protein expression normalized to that of the housekeeping protein glyceraldehyde-3-phosphate dehydrogenase (GAPDH) or α-tubulin. (*B*) Comparison of LATS2 and YAP1 basal expression determined by Western blot in AGS, MKN74, NCI-87, and Kato III human gastric epithelial cell lines. (*C*) Relative mRNA levels of YAP1 and LATS2 expression in siRNA transfected cells at 24 hours of HPI with *H pylori* 7.13 WT vs noninfected cells (ratio of mRNA levels in *H pylori*–infected cells vs noninfected cells). (*D*) TEAD-luciferase reporter activity in noninfected AGS and MKN74 cells at 30 hours after transfection with siCtrl, siLATS2, siYAP, pEGFP (control), pLATS2, pYAP1, and pYAP-S127A. (*E*) Quantification of the TEAD-luciferase reporter activity measured at 2 and 24 hours of HPI corresponding, respectively, to 8 and 30 hours after the last siRNA transfection in AGS and MKN74 cells. (*F*) Relative mRNA levels of CTGF and CYR61 expression in siRNA-transfected cells at 24 hours of HPI with WT *H pylori* vs noninfected cells (ratio of mRNA levels in *H pylori*–infected cells vs noninfected cells). (*C* and *F*) The *horizontal dotted lines* represent the level of the noninfected siControl cells. *Bars* represent the mean fold changes ± SEM, 3 < n < 6. *P < .05, **P < .01, ***P < .001, and ****P < .0001 vs siControl infected/noninfected cells using the Kruskal–Wallis test. #P < .05 vs noninfected siControls using Kruskal–Wallis test. (*D* and *E*) *Bars* represent the mean fold changes ± SEM, 3 < n < 6. *and #P < .05, **P < .01 vs respective noninfected siControl cells using the Kruskal–Wallis test. $Unavailable data. siCtrl, siControl.
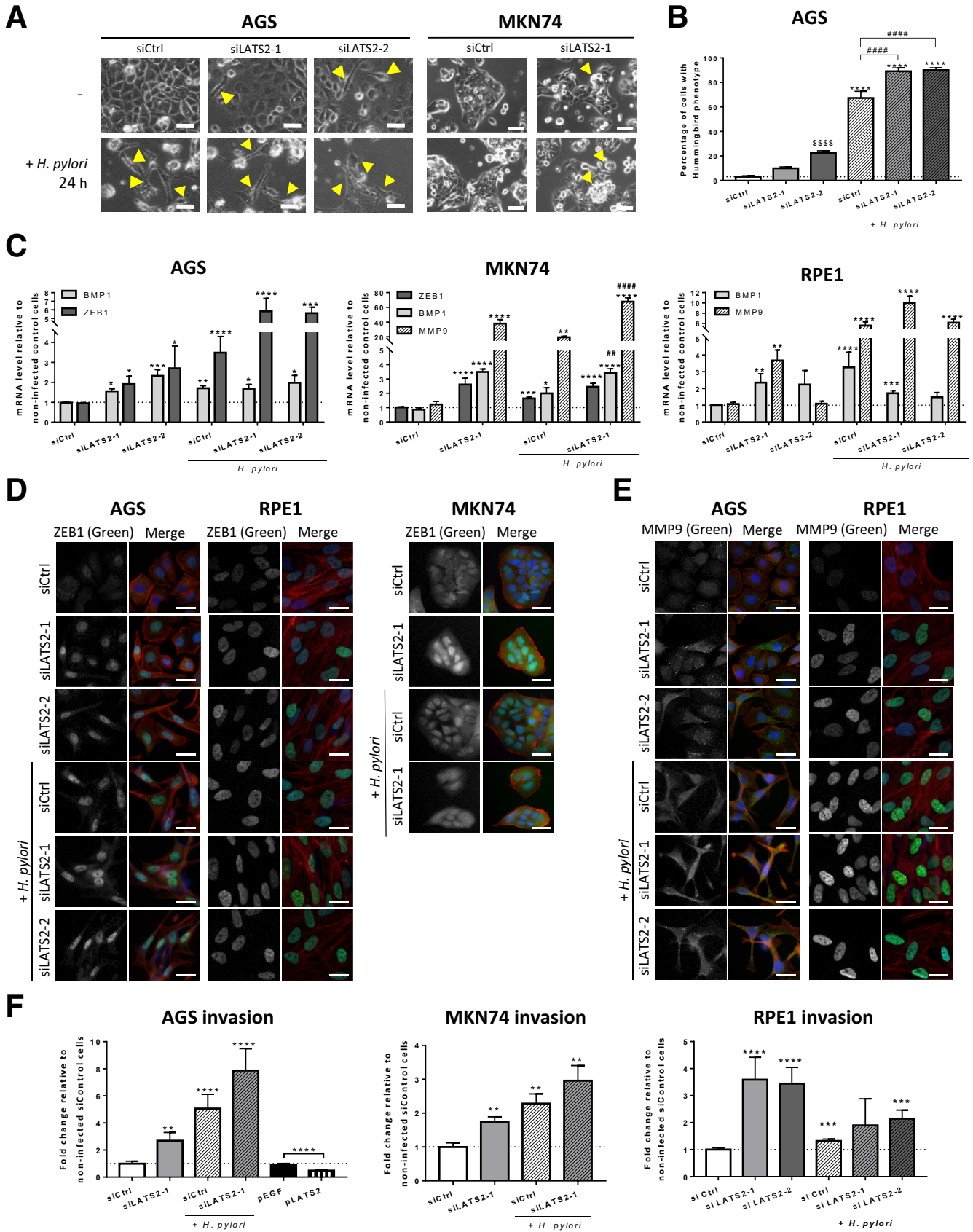
supplemented with 10% heat-inactivated fetal calf serum (all from Thermo Fisher Scientific, Courtaboeuf, France), at 37°C in a 5% CO_2 humidified atmosphere. The nontumorigenic, immortalized, human epithelial cell lines RPE1 (ATCC CRL-4000) and HMLE (kindly provided by R. Weinberg),[25] of retinal and mammary origin, respectively, were cultured in Dulbecco's modified Eagle medium/F12-Glutamax supplemented with 10% heat-inactivated fetal calf serum supplemented with 10 μg/mL insulin, 0.10 ng/mL epidermal growth factor, and 0.5 μg/mL hydrocortisone (all from Sigma-Aldrich, St. Quentin Fallavier, France) according to Mani et al[25] for the HMLE cell line. The experiments were performed with cells seeded at low density (2.5×10^4 cells/well in 24-well plates). Phase-contrast microscopy images of cell cultures were taken using an inverted phase-contrast Zeiss microscope equipped with a $\times$20 objective and a Zeiss acquisition software (Munich, Germany).

Bacterial Culture

H pylori strain 7.13 WT and its isogenic *cagA*-deleted mutant were cultured on Columbia agar plates at 37°C under microaerophilic (5% O_2) conditions, as previously described.[8,9] The coculture experiments were performed at a multiplicity of infection of 50.

Infection Experiments in Mice

Five-week-old C57BL/6J female mice were inoculated by oral gavage of the cagPAI and *cagA*-positive *H pylori* strain HPARE suspension every other day for 3 days, and 3–12 months later their stomach tissues were fixed and processed for standard histology as previously described.[9,19]

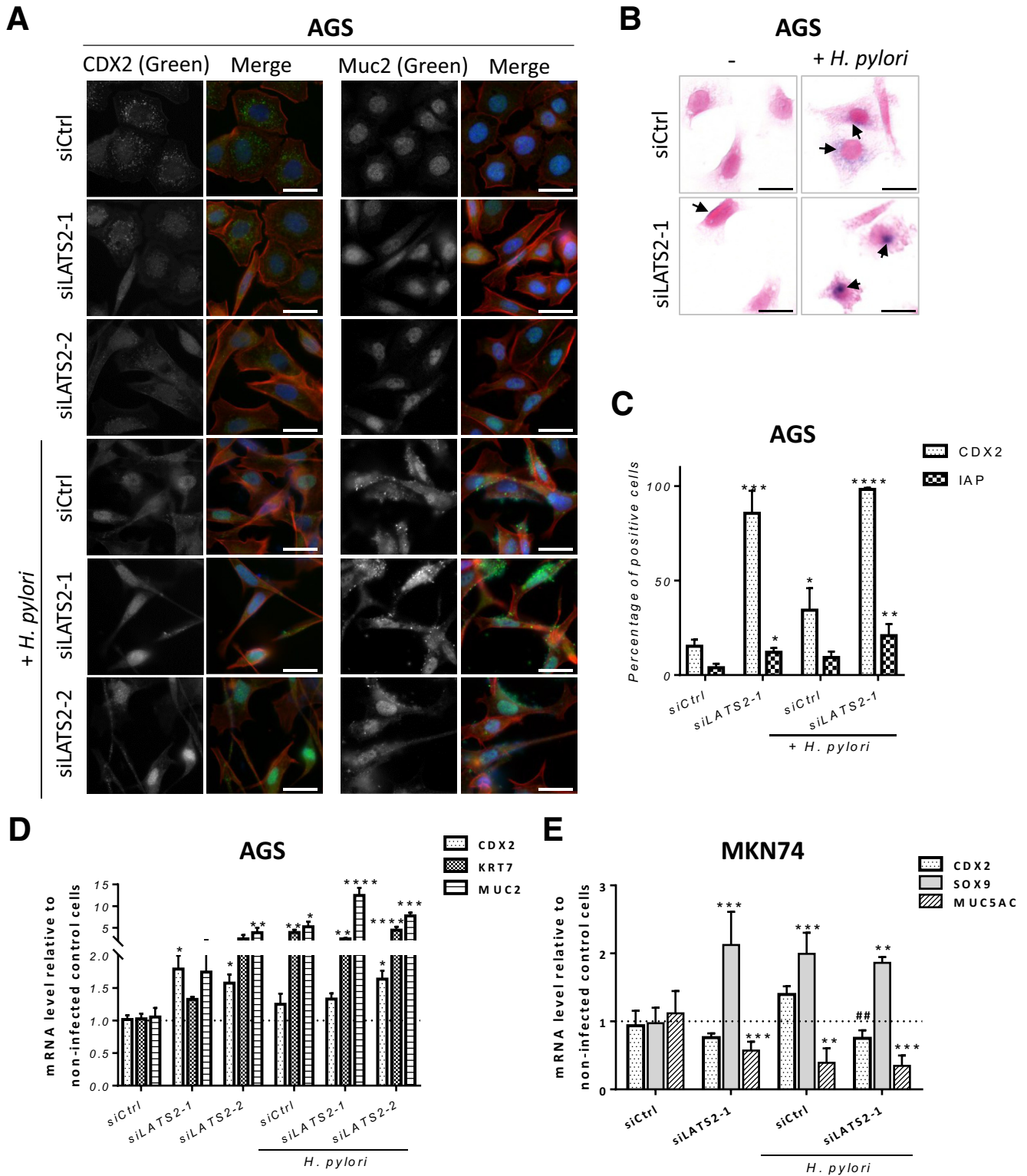### RNA Extraction, Transcriptome, and RT-qPCR

Cell RNAs were extracted using TRIzol reagent (Thermo Fisher Scientific) as recommended and quantified by their absorbance at 260 nm. For the transcriptome, RNAs were extracted using RNeasy (Qiagen, Courtaboeuf, France), and the RNA integrity number (RIN) were determined on the TapeStation (Agilent, Les Ulis, France). The transcriptome was performed with the GeTRix Platform

(Toulouse, France), and the Agilent G3 HGE 8 × 60 microarrays (Thermo Fisher Scientific). For RT-qPCR, the RT was performed with 1 μg total RNA using the Quantitect Reverse Transcription kit (Qiagen) as recommended. Quantitative PCR was performed using the SYBR-qPCR-Master mix (Promega, Lyon, France), with 0.3 μmol/L specific primers (LATS2 forward primer sequence CAGGATGCGACCAGGA-GATG and reverse primer sequence CCGCA-CAATCTGCTCATTC; YAP1 forward: CACAGCATGTTC GAGCTCAT, reverse: GATGCTGAGCTGTGGGTGTA; CTGF forward: GCCACAAGCTGTCCAGTCTAATCG, reverse: TGCATTCTCCAGCCATCAAGAGAC; CYR61 forward: ATGAATTGATTGCAGTTGGAAA, reverse: TAAAGGGTTGTA-TAGGATGCGA; ZEB1 forward: TCCCAACTTATGCCAGGCAC, reverse: CAGGAACCACATTTGTCATAGTCAC; Hypoxanthine Phosphoribosyltransferase 1 (HPRT1) forward: TGGTCA GGCAGTATAATCCA, reverse: GGTCCTTTTCACCAGCAAGCT; Tata-binding protein (TBP) forward: GGGCATTATTTGTG-CACTGAGA, reverse: GCCCAGATAGCAGCACGGT; CDX2 forward: GACGTGAGCATGTACCCTAGC, reverse: GCGTA GCCATTCCAGTCCT; SOX9 forward: CGGAGGAAGTCGGT-GAAG, reverse: CTGGGATTGCCCCGAGTGCT; and MUC2 forward: ACAACTACTCCTCTACCTCCA, reverse: GTTGATCTCGTAGTTGAGGCA; BMP1 Quantitect primer assay, cat. QT00000819; KRT7 Quantitect primer assay, cat. QT01672951; MMP9 Quantitect primer assay, cat. QT00040040; and MUC5AC Quantitect primer assay, cat. QT00088991) and 1:200 of the RT reaction volume. The amplification steps were as follows: 94°C for 15 seconds, 60°C for 30 seconds, and 72°C for 30 seconds, for 45 cycles. Relative expression was calculated using the comparative cycle treshold (Ct) method, with both HPRT1 and TBP as normalizers.

Transfection and Luciferase Reporter Assays

Cells were grown in 24-well plates and transfection of plasmids and siRNAs were performed using Lipofectamine 2000 and Lipofectamine RNAiMAX, respectively (Thermo Fisher Scientific) as recommended. Nonsilencing control siRNA (Allstars negative, cat. SI03650318; Qiagen) with no known homology to mammalian genes was used as a negative control. siRNA directed against human LATS2

Figure 6. (*See previous page*). **LATS2 restricts *H pylori*–induced EMT in AGS cells.** (*A*) Phase-contrast images of cells in siCtrl- and siLATS2-transfected cells upon 24 hours of HPI with *H pylori* 7.13 WT in AGS and MKN74. *Scale bars*: 20 μm. (a) In AGS cells (*left panel*), *Yellow arrows* indicate cells with the elongated hummingbird phenotype appearing in siLATS2 cells and at 24 hours of HPI. (b) In MKN74 cells (*right panel*), *Yellow arrows* indicate loosely attached round cell clusters appearing in siLATS2 cells infected or not infected. (*B*) Percentage of cells with the hummingbird phenotype in AGS cells. *P < .05 vs the respective noninfected condition. ****P < .0001 vs the respective noninfected condition. #### *P* < .0001 vs H. pylori–infected controls. $$$$ *P* < .0001 vs noninfected control cells in analysis of variance test. (*C*) Relative levels for the EMT markers ZEB1 (*dark grey bars*), BMP1 (*light grey bars*), MMP9 (*crosshatched bars*) mRNAs, measured at 24 hours of HPI with *H pylori* 7.13 WT in siControl-, siLATS2-1–, and siLATS2-2–transfected AGS, MKN74, and RPE1 cells. Bars represent the mean fold changes ± SEM of RT-qPCR data, 3 < n < 6. *P < .05, **P < .01, ***P < .001, ****P < .0001 vs noninfected siControl using the Kruskal–Wallis test. ##*P* < .01 vs *H pylori*–infected siControl using the Kruskal–Wallis test. (*D* and *E*) Expression and subcellular localization of (*D*) ZEB1 and (*E*) MMP9 (in green) assessed by immunofluorescence in AGS, RPE1, and MKN74 cells. F-actin was marked with Alexa-546–labeled phalloidin (red) and nuclei with 4'-6-diamino-phenyl-indol (blue). *Scale bars*: 10 μm. (*F*) Invasion capacity through collagen 1–coated Transwell inserts of *H pylori*–infected and noninfected siControl- and siLATS2-transfected AGS, MKN74, and RPE1 cells, and of noninfected pEGFP- (control) and pLATS2-transfected AGS cells, at 24 hours of HPI. Bars represent the mean fold changes ± SEM (n = 5) of the number of cells having crossed the Transwell 18 hours after plating, compared with noninfected siControl cells. **P < .01, ***P < .001, and ****P < .0001 vs noninfected siControl using the Kruskal–Wallis test. siCtrl, siControl.

A AGS

CDX2 (Green) | Merge | Muc2 (Green) | Merge

siCtrl / siLATS2-1 / siLATS2-2

+ H. pylori: siCtrl / siLATS2-1 / siLATS2-2

B AGS

- | + H. pylori

siCtrl / siLATS2-1

C AGS

Percentage of positive cells

CDX2 / IAP

D AGS

mRNA level relative to non-infected control cells

CDX2 / KRT7 / MUC2

siCtrl / siLATS2-1 / siLATS2-2 / siCtrl / siLATS2-1 / siLATS2-2

H. pylori

E MKN74

mRNA level relative to non-infected control cells

CDX2 / SOX9 / MUC5AC

siCtrl / siLATS2-1 / siCtrl / siLATS2-1

H. pylori

(LATS2-1, cat. GS26524; Qiagen; and LATS2-2, cat. SO-2702484G/M-003865-02-0005, Dharmacon, Denver, CO) and YAP1 (YAP1-1, cat. GS10413; Qiagen; and YAP1-2, sequence 5'-UGUGGAUGAGAUGGAUAGA-3', Eurofins, Dortmund, Germany) were used at 20 nmol/L; 2 rounds of

siRNA transfection were performed. The TEAD (8 × GTII-luciferase was a gift from Stefano Piccolo[25]) or TATA box control (transcription-activator like [TAL], BectonDickinson, Le Pont de Claix, France) firefly luciferase reporters were transfected at 100 ng/well, in the presence of 10 ng/well

Renilla luciferase reporter (pRL-SV40; Promega). Firefly and Renilla luciferase activities were measured using the Dual Luciferase Assay (Promega). Firefly luciferase activities were normalized for transfection efficiency by Renilla luciferase for each sample, and TEAD-specific luciferase activity then was normalized to that of TAL. The expression vectors plasmid cloning desoxyribonucleic acid (pcDNA)-Flag-YAP1, plasmid with Cytomegalovirus promoter (pCMV)-flagS127A-YAP1, and pCMVmyc-LATS2 vectors were generous gifts from Yosef Shaul,[40] Kunliang Guan,[41] and Professor H Nojima, Osaka, Japan,[7] respectively); the control pEGFP-C3 vector was from Promega. The expression vectors were transfected at 500 ng/well.

Western Blot

Cells were lysed on ice in ProteoJET reagent (Thermo Fisher Scientific) supplemented with a protease/phosphatase inhibitor cocktail (Sigma-Aldrich). The extracted proteins were submitted to sodium dodecyl sulfate–polyacrylamide gel electrophoresis and Western blot on Protean nitrocellulose membranes (Amersham, Orsay, France) for immunolabeling. Immunolabeling was performed using rabbit anti-YAP1, anti–YAP1-P^{Ser127}, and anti–LATS1/2-P$^{Thr1079/1041}$ (each at 1:2000, cat. 4912, cat. 4911, and cat. 8654, respectively; Cell Signaling Technology, Ozyme, St. Quentin-en-Yvelines, France), rabbit anti-LATS1/2 (1:2000, cat. A300-479; Bethyl, Souffelweyersheim, France), mouse anti–α-tubulin (1:8000; cat. T-6074, Sigma-Aldrich), mouse anti–glyceraldehyde-3-phosphate dehydrogenase (1:2000, sc-47724; Santa Cruz Biotechnology, Heidelberg, Germany), followed by horseradish-peroxidase–coupled, anti-rabbit and anti-mouse secondary antibodies (DAKO, Les Ulis, France) and chemoluminescent detection (ECL+, Amersham). The band intensities relative to α-tubulin or glyceraldehyde-3-phosphate dehydrogenase were quantified using ImageJ software (National Institutes of Health, Bethesda, MD).

Immunocytofluorescence

Cells (2.5×10^4) cultured on glass coverslips were fixed in a 4% paraformaldehyde solution in phosphate-buffered saline supplemented with 1 mmol/L CaCl$_2$ and 1 mmol/L MgCl$_2$ (Ca-Mg) for 10 minutes and permeabilized in 0.1% Triton X-100 (Sigma-Aldrich, Lyon, France) in Tris-Buffered Saline (TBS)-Ca-Mg for 1 minute at room temperature. After blocking with 1% bovine serum albumin, 2% fetal calf serum solution in TBS-Ca-Mg, they were incubated stepwise with either a rabbit anti-LATS1/2 (1:200 dilution, Bethyl),

anti-YAP1 (1:100, Cell Signaling), anti–YAP1-P^{Ser127} (1:200, Cell Signaling), anti-ZEB1 (1:100, cat. A301-922, Bethyl), anti-Mucin 2 (1:50, cat. sc-15334, Santa Cruz Biotechnology), a mouse anti-CDX2 (prediluted ready to use, CDX2-88 ab86949; Abcam, Paris, France), anti-MMP9 (1:100, H-300, sc-21733, Santa Cruz Technology) antibody for 1 hour at room temperature, followed by a goat anti-rabbit Alexa-488–labeled secondary antibody (1:250, cat. A32731; Thermo Fisher Scientific) or a donkey anti-mouse Alexa-488–labeled secondary antibody (1:250, cat A21202, Thermo Fisher Scientific) mixed to Alexa-546–labeled phalloidin (1:250, cat. A22283, Thermo Fisher Scientific) and 4'-6-diamino-phenyl-indol (50 mg/mL, cat. D9542; Sigma-Aldrich) for 1 hour at room temperature. The coverslips were mounted on glass slides using Slowfade reagent (S36936; Thermo Fisher Scientific). Images were taken using an Eclipse 50i epi-fluorescence microscope (Nikon, Champigny sur Marne, France) with Nis Element acquisition software and a ×40 (numeric aperture, 1.3) oil immersion objective.

Cytology and Immunocytology

Cells were cultured and processed as for immunostaining. Alkaline phosphatase activity was detected by the 5-bromo-4-chloro-3-indolyl-phosphate/nitroblue tetrazolium (BCIP/NBT) Alkaline Phosphatase Substrate Kit IV, following the manufacturer's instructions (Vector Laboratories, Interchim, Montluçon, France) and slides were counterstained with nuclear fast red, dehydrated, and mounted on slides with Eukitt-mounting medium (VWR, Fontenay-sous-Bois, France).[19]

Invasion Assay

Cells were recovered by trypsinization and 2.5×10^4 cells per condition were placed in the upper side of a 8-μm pore size Corning Transwell (Sigma-Aldrich) insert, previously coated with rat-tail type 1 collagen (Becton Dickinson), in 24-well culture plates with medium containing 5% fetal bovine serum. After 18 hours of incubation at 37°C, the Transwell inserts were fixed in 4% paraformaldehyde solution and labeled with 4'-6-diamino-phenyl-indol. Cells from the upper part of the Transwell inserts were removed by swabbing and cells that invaded through the lower side of the inserts were counted on 5 different randomly chosen fields per insert under microscopy with the ZOE fluorescent Cell Imager (BioRad, Marnes-la-Coquette, France).

Figure 7. (*See previous page*). **LATS2 controls *H pylori*–elicited metaplasia.** (*A*) Expression and subcellular localization of CDX2 and MUC2, assessed by immunofluorescent staining (in green) in AGS cells. F-actin was stained with Alexa-546–labeled phalloidin (in red) and nuclei with 4'-6-diamino-phenyl-indol (in blue). *Scale bars*: 10 μm. (*B*) The IAP activity, assessed by BCIP/NBT transformation (cytoplasmic dark blue foci) and countercoloration by nuclear fast red, in AGS cells at 24 hours of HPI. *Scale bars*: 10 μm. *Black arrows* indicate IAP activity detected as dark blue foci in AGS cells. (*C*) Quantification of the percentage of positive cells for CDX2 (*white dotted bars*) and IAP (*grid bars*) by light microscopy observation. *Bars* represent the mean fold changes ± SD, n = 3. *$P < .05$, **$P < .01$, ***$P < .001$, and ****$P < .0001$ vs noninfected siControl cells using analysis of variance. (*D* and *E*) Relative expression of CDX2, KRT7, MUC2, SOX9, and MUC5AC mRNA; bars represent the mean fold changes ± SEM of RT-qPCR data, n = 3. *$P < .05$, **$P < .01$, ***$P < .001$, and ****$P < .0001$ vs noninfected siControl cells using the Kruskal–Wallis test. ##$P < .01$ vs *H pylori*–infected siControl using the Kruskal–Wallis test.

Immunohistochemistry

Tissue sections (3-μm thick) were prepared from formalin-fixed, paraffin-embedded human tissues and underwent standard immunohistochemistry protocols for LATS2 (rabbit anti-LATS1/2, 1:100, 2 h; Bethyl), YAP1 (rabbit anti-YAP1, 1:100, 1 h; Cell Signaling), or *H pylori* (rabbit anti–*H pylori* 1:100, 2 h, cat. B0471; DAKO) antibodies, and then with horseradish-peroxidase–labeled anti-rabbit EnVision System (30 min; DAKO).[17] Immunolabeling was shown after a 10-minute incubation in liquid diaminobenzidine-chromogen substrate (cat. K3468; DAKO). Slides were counterstained with hematoxylin, dehydrated, and mounted with Eukitt-mounting medium (VWR). Relative quantification of the percentage of gastric epithelial cells expressing nuclear LATS2 and nuclear YAP1 was determined by a double-blind scoring using a scale from 1 to 4 (0, 0%; 1, <5%; 2, 5%–25%; 3, 25%–50%; and 4, >50%).

Statistical Analysis

Quantification values represent the means of 3 or more independent experiments, each performed by triplicate or more ± SEM. The Mann–Whitney test was used to compare between 2 groups and the Kruskal–Wallis test with the Dunn posttest or analysis of variance tests and Bonferroni post hoc test were used for multiple comparisons. Statistics were performed on GraphPad Prism 7.02 software (San Diego, CA, USA).

References

1. Correa P, Houghton J. Carcinogenesis of Helicobacter pylori. Gastroenterology 2007;133:659–672.
2. Bray F, Jemal A, Grey N, Ferlay J, Forman D. Global cancer transitions according to the Human Development Index (2008-2030): a population-based study. Lancet Oncol 2012;13:790–801.
3. Backert S, Selbach M. Role of type IV secretion in Helicobacter pylori pathogenesis. Cell Microbiol 2008; 10:1573–1581.
4. Megraud F, Bessede E, Varon C. Helicobacter pylori infection and gastric carcinoma. Clin Microbiol Infect 2015;21:984–990.
5. Mimuro H, Suzuki T, Nagai S, Rieder G, Suzuki M, Nagai T, Fujita Y, Nagamatsu K, Ishijima N, Koyasu S, Haas R, Sasakawa C. Helicobacter pylori dampens gut epithelial self-renewal by inhibiting apoptosis, a bacterial strategy to enhance colonization of the stomach. Cell Host Microbe 2007;2:250–263.
6. Hatakeyama M. Helicobacter pylori and gastric carcinogenesis. J Gastroenterol 2009;44:239–248.
7. Belair C, Baud J, Chabas S, Sharma CM, Vogel J, Staedel C, Darfeuille F. Helicobacter pylori interferes with an embryonic stem cell micro RNA cluster to block cell cycle progression. Silence 2010;2:7.
8. Baud J, Varon C, Chabas S, Chambonnier L, Darfeuille F, Staedel C. Helicobacter pylori initiates a mesenchymal transition through ZEB1 in gastric epithelial cells. PLoS One 2013;8:e60315.
9. Bessede E, Staedel C, Acuna Amador LA, Nguyen PH, Chambonnier L, Hatakeyama M, Belleannee G, Megraud F, Varon C. Helicobacter pylori generates cells with cancer stem cell properties via epithelial-mesenchymal transition-like changes. Oncogene 2014;33:4123–4131.
10. Thiery JP, Acloque H, Huang RY, Nieto MA. Epithelial-mesenchymal transitions in development and disease. Cell 2009;139:871–890.
11. Yu FX, Zhao B, Guan KL. Hippo pathway in organ size control, tissue homeostasis, and cancer. Cell 2015; 163:811–828.
12. Piccolo S, Dupont S, Cordenonsi M. The biology of YAP/TAZ: hippo signaling and beyond. Physiol Rev 2014; 94:1287–1312.
13. Hansen CG, Moroishi T, Guan KL. YAP and TAZ: a nexus for Hippo signaling and beyond. Trends Cell Biol 2015; 25:499–513.
14. Zanconato F, Cordenonsi M, Piccolo S. YAP/TAZ at the roots of cancer. Cancer Cell 2016;29:783–803.
15. Kang W, Tong JH, Chan AW, Lee TL, Lung RW, Leung PP, So KK, Wu K, Fan D, Yu J, Sung JJ, To KF. Yes-associated protein 1 exhibits oncogenic property in gastric cancer and its nuclear accumulation associates with poor prognosis. Clin Cancer Res 2011;17:2130–2139.
16. Song M, Cheong JH, Kim H, Noh SH, Kim H. Nuclear expression of Yes-associated protein 1 correlates with poor prognosis in intestinal type gastric cancer. Anticancer Res 2012;32:3827–3834.
17. Yu L, Gao C, Feng B, Wang L, Tian X, Wang H, Ma D. Distinct prognostic values of YAP1 in gastric cancer. Tumour Biol 2017;39:1010428317695926.
18. Bessede E, Dubus P, Megraud F, Varon C. Helicobacter pylori infection and stem cells at the origin of gastric cancer. Oncogene 2015;34:2547–2555.
19. Varon C, Dubus P, Mazurier F, Asencio C, Chambonnier L, Ferrand J, Giese A, Senant-Dugot N, Carlotti M, Megraud F. Helicobacter pylori infection recruits bone marrow-derived cells that participate in gastric preneoplasia in mice. Gastroenterology 2012; 142:281–291.
20. Bessede E, Molina S, Amador LA, Dubus P, Staedel C, Chambonnier L, Buissonniere A, Sifre E, Giese A, Benejat L, Rousseau B, Costet P, Sacks DB, Megraud F, Varon C. Deletion of IQGAP1 promotes Helicobacter pylori-induced gastric dysplasia in mice and acquisition of cancer stem cell properties in vitro. Oncotarget 2016; 7:80688–80699.
21. Jiao S, Li C, Hao Q, Miao H, Zhang L, Li L, Zhou Z. VGLL4 targets a TCF4-TEAD4 complex to coregulate Wnt and Hippo signalling in colorectal cancer. Nat Commun 2017;8:14058.
22. Szymaniak AD, Mahoney JE, Cardoso WV, Varelas X. Crumbs3-mediated polarity directs airway epithelial cell fate through the Hippo pathway effector Yap. Dev Cell 2015;34:283–296.
23. Tanaka I, Osada H, Fujii M, Fukatsu A, Hida T, Horio Y, Kondo Y, Sato A, Hasegawa Y, Tsujimura T, Sekido Y. LIM-domain protein AJUBA suppresses malignant mesothelioma cell proliferation via Hippo signaling cascade. Oncogene 2015;34:73–83.

24. Philippe C, Pinson B, Dompierre J, Pantesco V, Viollet B, Daignan-Fornier B, Moenner M. AICAR antiproliferative properties involve the AMPK-independent activation of the tumor suppressors LATS 1 and 2. Neoplasia 2018; 20:555–562.

25. Mani SA, Guo W, Liao MJ, Eaton EN, Ayyanan A, Zhou AY, Brooks M, Reinhard F, Zhang CC, Shipitsin M, Campbell LL, Polyak K, Brisken C, Yang J, Weinberg RA. The epithelial-mesenchymal transition generates cells with properties of stem cells. Cell 2008;133:704–715.

26. von Eyss B, Jaenicke LA, Kortlever RM, Royla N, Wiese KE, Letschert S, McDuffus LA, Sauer M, Rosenwald A, Evan GI, Kempa S, Eilers M. A MYC-driven change in mitochondrial dynamics limits YAP/TAZ function in mammary epithelial cells and breast cancer. Cancer Cell 2015;28:743–757.

27. Barros R, Freund JN, David L, Almeida R. Gastric intestinal metaplasia revisited: function and regulation of CDX2. Trends Mol Med 2012;18:555–563.

28. Yamamoto H, Bai YQ, Yuasa Y. Homeodomain protein CDX2 regulates goblet-specific MUC2 gene expression. Biochem Biophys Res Commun 2003;300:813–818.

29. Goldberg RF, Austen WG Jr, Zhang X, Munene G, Mostafa G, Biswas S, McCormack M, Eberlin KR, Nguyen JT, Tatlidede HS, Warren HS, Narisawa S, Millan JL, Hodin RA. Intestinal alkaline phosphatase is a gut mucosal defense factor maintained by enteral nutrition. Proc Natl Acad Sci U S A 2008;105:3551–3556.

30. Zhang X, Shi D, Liu YP, Chen WJ, Wu D. Effects of the Helicobacter pylori virulence factor CagA and ammonium ion on mucins in AGS cells. Yonsei Med J 2018; 59:633–642.

31. Serizawa T, Hirata Y, Hayakawa Y, Suzuki N, Sakitani K, Hikiba Y, Ihara S, Kinoshita H, Nakagawa H, Tateishi K, Koike K. Gastric metaplasia induced by Helicobacter pylori is associated with enhanced SOX9 expression via interleukin-1 signaling. Infect Immun 2016;84:562–572.

32. Yi J, Lu L, Yanger K, Wang W, Sohn BH, Stanger BZ, Zhang M, Martin JF, Ajani JA, Chen J, Lee JS, Song S, Johnson RL. Large tumor suppressor homologs 1 and 2 regulate mouse liver progenitor cell proliferation and maturation through antagonism of the coactivators YAP and TAZ. Hepatology 2016;64:1757–1772.

33. Park GS, Oh H, Kim M, Kim T, Johnson RL, Irvine KD, Lim DS. An evolutionarily conserved negative feedback mechanism in the Hippo pathway reflects functional difference between LATS1 and LATS2. Oncotarget 2016; 7:24063–24075.

34. Barry ER, Camargo FD. The Hippo superhighway: signaling crossroads converging on the Hippo/Yap pathway in stem cells and development. Curr Opin Cell Biol 2013;25:247–253.

35. Ramos A, Camargo FD. The Hippo signaling pathway and stem cell biology. Trends Cell Biol 2012;22:339–346.

36. Furth N, Aylon Y. The LATS1 and LATS2 tumor suppressors: beyond the Hippo pathway. Cell Death Differ 2017;24:1488–1501.

37. Moroishi T, Park HW, Qin B, Chen Q, Meng Z, Plouffe SW, Taniguchi K, Yu FX, Karin M, Pan D, Guan KL. A YAP/TAZ-induced feedback mechanism regulates Hippo pathway homeostasis. Genes Dev 2015; 29:1271–1284.

38. Kulkarni M, Tan TZ, Syed Sulaiman NB, Lamar JM, Bansal P, Cui J, Qiao Y, Ito Y. RUNX1 and RUNX3 protect against YAP-mediated EMT, stem-ness and shorter survival outcomes in breast cancer. Oncotarget 2018; 9:14175–14192.

39. Qiao Y, Lin SJ, Chen Y, Voon DC, Zhu F, Chuang LS, Wang T, Tan P, Lee SC, Yeoh KG, Sudol M, Ito Y. RUNX3 is a novel negative regulator of oncogenic TEAD-YAP complex in gastric cancer. Oncogene 2016;35:2664–2674.

40. Levy D, Adamovich Y, Reuven N, Shaul Y. The Yes-associated protein 1 stabilizes p73 by preventing Itch-mediated ubiquitination of p73. Cell Death Differ 2007; 14:743–751.

41. Zhao B, Wei X, Li W, Udan RS, Yang Q, Kim J, Xie J, Ikenoue T, Yu J, Li L, Zheng P, Ye K, Chinnaiyan A, Halder G, Lai ZC, Guan KL. Inactivation of YAP oncoprotein by the Hippo pathway is involved in cell contact inhibition and tissue growth control. Genes Dev 2007;21:2747–2761.

42. Li W, Cooper J, Zhou L, Yang C, Erdjument-Bromage H, Zagzag D, Snuderl M, Ladanyi M, Hanemann CO, Zhou P, Karajannis MA, Giancotti FG. Merlin/NF2 loss-driven tumorigenesis linked to CRL4(DCAF1)-mediated inhibition of the hippo pathway kinases Lats1 and 2 in the nucleus. Cancer Cell 2014;26:48–60.

43. Enderle L, McNeill H. Hippo gains weight: added insights and complexity to pathway control. Sci Signal 2013;6:re7.

44. Murata-Kamiya N, Kurashima Y, Teishikata Y, Yamahashi Y, Saito Y, Higashi H, Aburatani H, Akiyama T, Peek RM Jr, Azuma T, Hatakeyama M. Helicobacter pylori CagA interacts with E-cadherin and deregulates the beta-catenin signal that promotes intestinal transdifferentiation in gastric epithelial cells. Oncogene 2007;26:4617–4626.

45. Amieva MR, Vogelmann R, Covacci A, Tompkins LS, Nelson WJ, Falkow S. Disruption of the epithelial apical-junctional complex by Helicobacter pylori CagA. Science 2003;300:1430–1434.

46. Hatakeyama M. Helicobacter pylori CagA and gastric cancer: a paradigm for hit-and-run carcinogenesis. Cell Host Microbe 2014;15:306–316.

47. Coulombe G, Rivard N. New and unexpected biological functions for the Src-homology 2 domain-containing phosphatase SHP-2 in the gastrointestinal tract. Cell Mol Gastroenterol Hepatol 2011;2:11–21.

48. Tsutsumi R, Masoudi M, Takahashi A, Fujii Y, Hayashi T, Kikuchi I, Satou Y, Taira M, Hatakeyama M. YAP and TAZ, Hippo signaling targets, act as a rheostat for nuclear SHP2 function. Dev Cell 2013;26:658–665.

49. Yamazaki S, Yamakawa A, Ito Y, Ohtani M, Higashi H, Hatakeyama M, Azuma T. The CagA protein of Helicobacter pylori is translocated into epithelial cells and binds to SHP-2 in human gastric mucosa. J Infect Dis 2003;187:334–337.

50. Lehmann W, Mossmann D, Kleemann J, Mock K, Meisinger C, Brummer T, Herr R, Brabletz S, Stemmler MP, Brabletz T. ZEB1 turns into a

transcriptional activator by interacting with YAP1 in aggressive cancer types. Nat Commun 2016;7:10498.

51. Yao F, Liu H, Li Z, Zhong C, Fang W. Down-regulation of LATS2 in non-small cell lung cancer promoted the growth and motility of cancer cells. Tumour Biol 2015; 36:2049–2057.

52. Furth N, Bossel Ben-Moshe N, Pozniak Y, Porat Z, Geiger T, Domany E, Aylon Y, Oren M. Down-regulation of LATS kinases alters p53 to promote cell migration. Genes Dev 2015;29:2325–2330.

53. Cobler L, Pera M, Garrido M, Iglesias M, de Bolos C. CDX2 can be regulated through the signalling pathways activated by IL-6 in gastric cells. Biochim Biophys Acta 2014;1839:785–792.

54. Camilo V, Barros R, Sousa S, Magalhaes AM, Lopes T, Mario Santos A, Pereira T, Figueiredo C, David L, Almeida R. Helicobacter pylori and the BMP pathway regulate CDX2 and SOX2 expression in gastric cells. Carcinogenesis 2012;33:1985–1992.

55. Naumann M, Sokolova O, Tegtmeyer N, Backert S. Helicobacter pylori: a paradigm pathogen for subverting host cell signal transmission. Trends Microbiol 2017; 25:316–328.

Correspondence
Address correspondence to: Christine Varon, PhD, INSERM U1053 Bordeaux Research in Translational Oncology (BaRITOn), University of Bordeaux, 146 Rue Léo Saignat, 33076 Bordeaux Cedex, France. e-mail: christine.varon@u-bordeaux.fr; fax: +33 5 56 79 60 18; or Cathy Staedel, PhD, INSERM U1212, "ARN: Régulations naturelle et artificielle" (ARNA)-Unités Mixtes de Recherche (UMR) Centre national de la recherche scientifique (CNRS) 5320, University of Bordeaux, 146 Rue Léo Saignat, 33076 Bordeaux Cedex, France. e-mail: cathy.staedel@inserm.fr; fax: +33 5 57 57 10 15.

Author contributions
Silvia Elena Molina Castro acquired, analyzed, and interpreted the data, performed the statistical analysis, and drafted the manuscript; Julie Giraud and Camille Tiffon acquired, analyzed, and interpreted the data, and performed the statistical analysis; Elodie Sifre and Alban Giese provided technical support; Geneviève Belleannée and Hélène Boeuf provided material support; Hélène Boeuf, Emilie Bessède, Philippe Lehours, Francis Mégraud, and Pierre Dubus critically revised the manuscript for important intellectual content; Cathy Staedel was responsible for the study concept, acquired, analyzed, and interpreted the data, and drafted the manuscript; and Christine Varon was responsible for the study concept, analyzed and interpreted the data, designed and supervised the study, drafted the manuscript, and obtained funding.

Conflicts of interest
The authors disclose no conflicts.